Chem. Rev. **2005,** *105,* 1547–1562

Nanostructures in Biodiagnostics

Nathaniel L. Rosi and Chad A. Mirkin*

Chapter 19

Nanomaterials for Biodiagnostic

- Nucleic Acid
  - Genetic information for identification
  - Diseases, bacterium, virus, pathogen
  - PCR with molecular fluorophore, State of the Art
  - Expansive, Non-portable, Non-multiplexing
- Proteins
  - Cancers and diseases, unusual high concentration of marker
  - ELISA (~pM) with molecular fluorophore
  - No PCR version

10 ppb $\frac{10\ ng}{1\ g}$ ~ 1 PSA long / c.c.

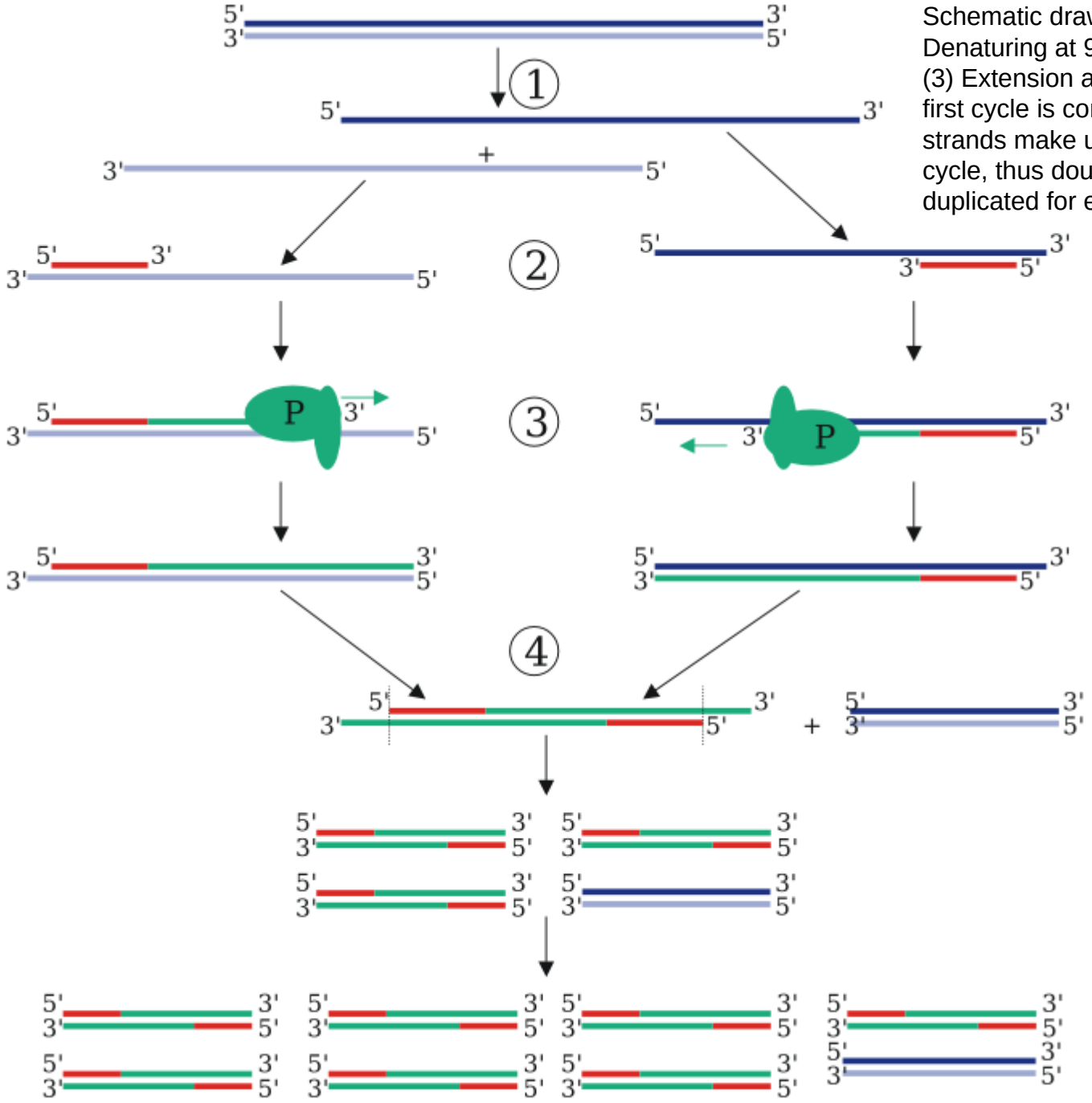

Schematic drawing of the PCR cycle. (1) Denaturing at 94-96˚C. (2) Annealing at (eg) 68˚C. (3) Extension at 72˚C (P=Polymerase). (4) The first cycle is complete. The two resulting DNA strands make up the template DNA for the next cycle, thus doubling the amount of DNA duplicated for each new cycle.

PCR for Forensic Science

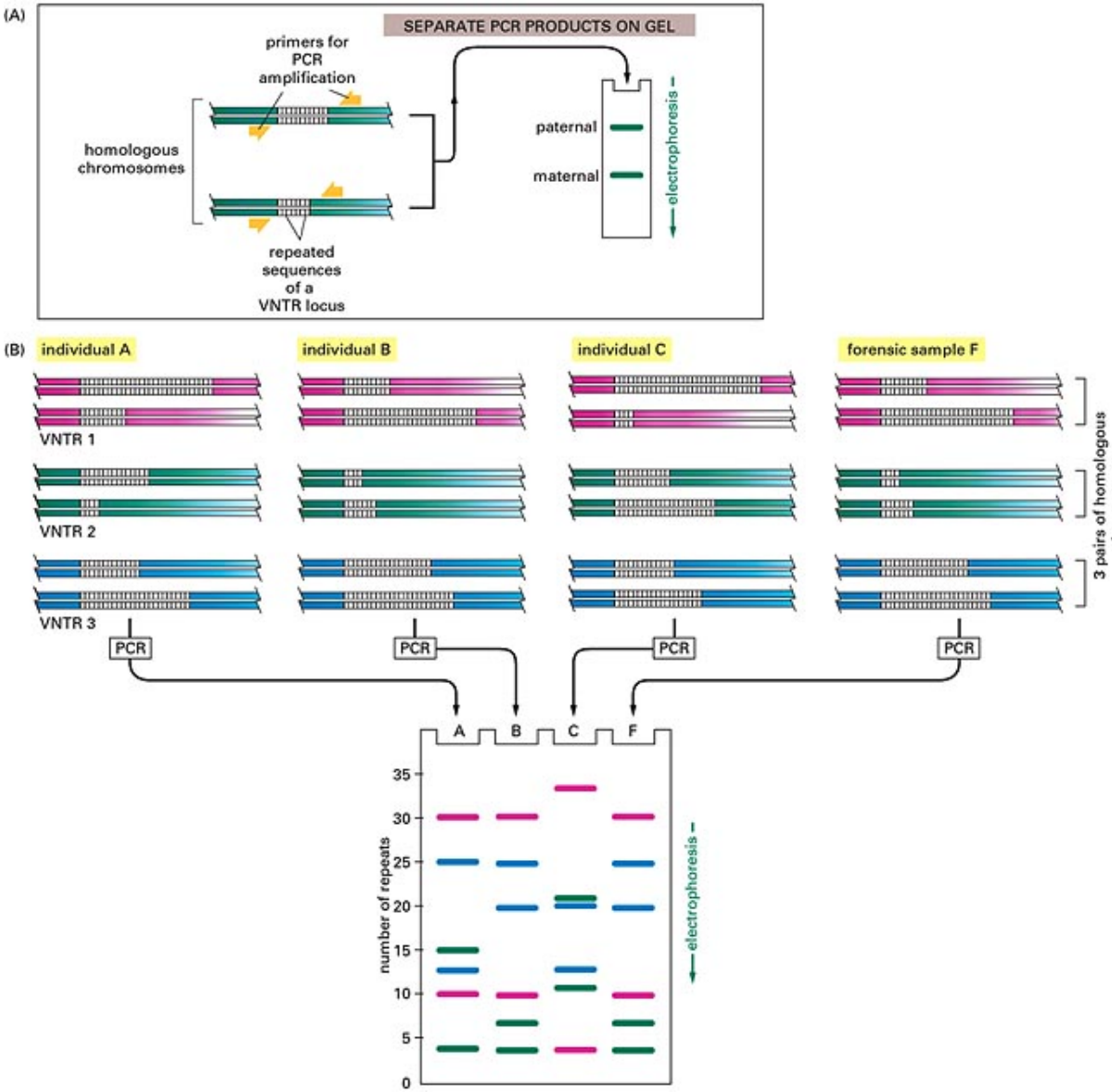

(A) The DNA sequences that create the variability used in this analysis contain runs of short, repeated sequences, such as GTGTGT . . . , which are found in various positions (loci) in the human genome. The number of repeats in each run is highly variable in the population, ranging from 4 to 40 in different individuals. A run of repeated nucleotides of this type is commonly referred to as a VNTR (variable number of tandem repeat) sequence. Because of the variability in these sequences, each individual will usually inherit a different variant of each VNTR locus from their mother and from their father; two unrelated individuals will therefore not usually contain the same pair of sequences. A PCR reaction using primers that bracket the locus produces a pair of bands of amplified DNA from each individual, one band representing the maternal variant and the other representing the paternal variant. The length of the amplified DNA, and thus its position after electrophoresis, will depend on the exact number of repeats at the locus. (B) The DNA bands obtained from a set of four different PCR reactions, each of which amplifies the DNA from a different VNTR locus. In the schematic example shown here, the same three VNTR loci are analyzed from three suspects (individuals A, B, and C), giving six bands for each person. You can see that although some individuals have several bands in common, the overall pattern is quite distinctive for each. The band pattern can serve as a ³fingerprint² to identify an individual nearly uniquely. The fourth lane (F) contains the products of the same PCR reactions carried out on a forensic sample. The starting material for such a PCR reaction can be a single hair that was left at the scene of the crime. From the example, individuals A and C can be eliminated from enquiries, while B remains a clear suspect.

ELISA (Enzyme-Linked Immunosorbent Assay)

is a biochemical technique used mainly in immunology to detect the presence of an antibody or an antigen in a sample. It utilizes two antibodies, one of which is specific to the antigen and the other of which is coupled to an enzyme. This second antibody gives the assay its "enzyme-linked" name, and will cause a chromogenic or fluorogenic substrate to produce a signal.

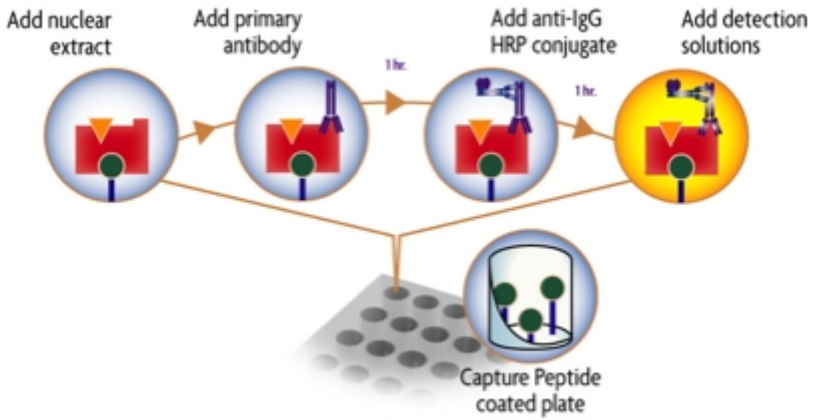

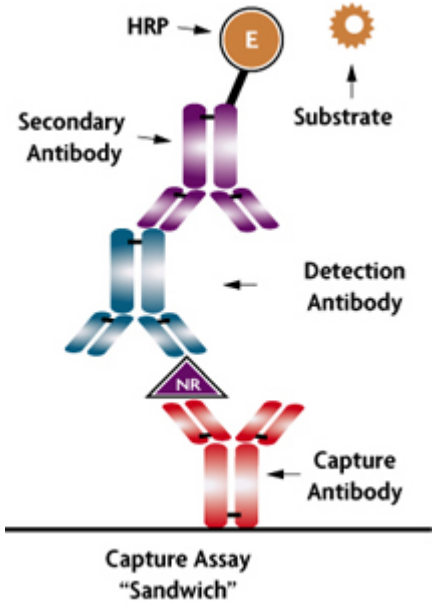

Why Nanomaterials?

- Molecular fluorophores
  - Limited spectral response
  - photostability
- Nanomaterials
  - Small size (1-100 nm)
  - Chemically tailorable physical properties
  - Unusual target binding properties
  - Structure robustness

Tailorable Physical Properties

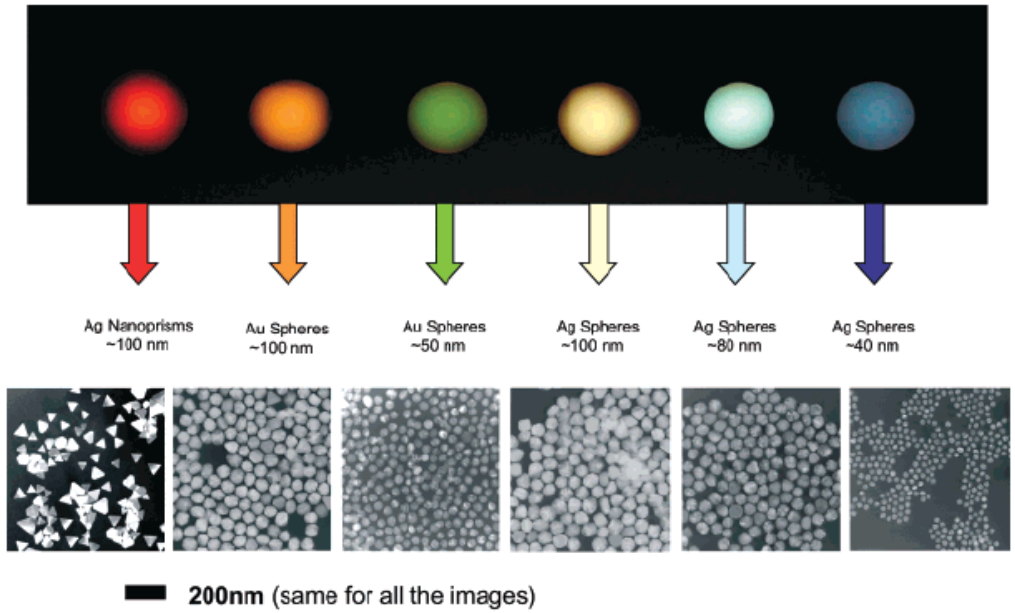

Figure 1. Sizes, shapes, and compositions of metal nanoparticles can be systematically varied to produce materials with distinct light-scattering properties.

Nanomaterial Detection

- Optical
- Electrical and electrochemical
- Magnetic
- Nanowire and Nanotubes
- Nanofabrication

Colorimetric Detection of DNA

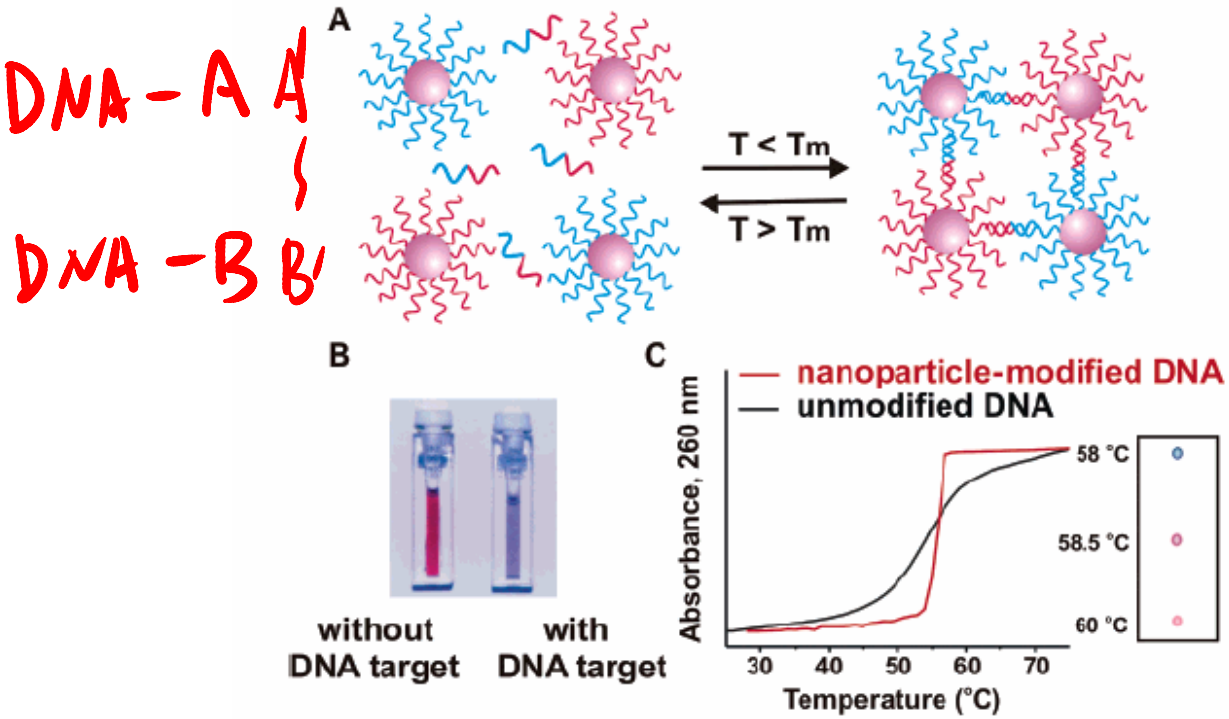

Figure 2. In the presence of complementary target DNA, oligonucleotide-functionalized gold nanoparticles will aggregate (A), resulting in a change of solution color from red to blue (B). The aggregation process can be monitored using UV−vis spectroscopy or simply by spotting the solution on a silica support (C). (Reprinted with permission from *Science* (http://www.aaas.org), ref 29. Copyright 1997 American Association for the Advancement of Science.)

A DNA-based method for rationally assembling nanoparticles into macroscopic materials

Chad A. Mirkin, Robert L. Letsinger, Robert C. Mucic & James J. Storhoff

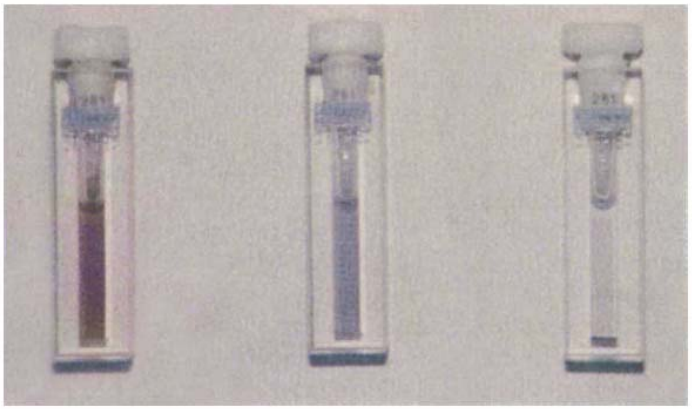

FIG. 2 Cuvettes with the Au colloids and the four DNA strands responsible for the assembly process. Left cuvette, at 80 °C with DNA-modified colloids in the unhybridized state; centre, after cooling to room temperature but before the precipitate settles; and right, after the polymeric precipitate settles to the bottom of the cuvette. Heating either of these cool solutions results in the reformation of the DNA-modified colloids in the unhybridized state (shown in the left cuvette).

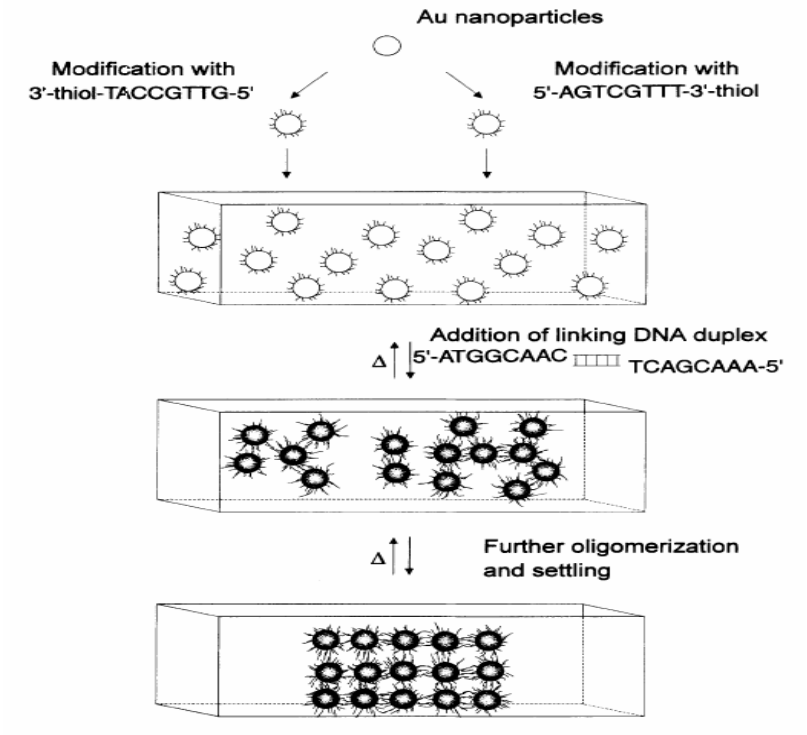

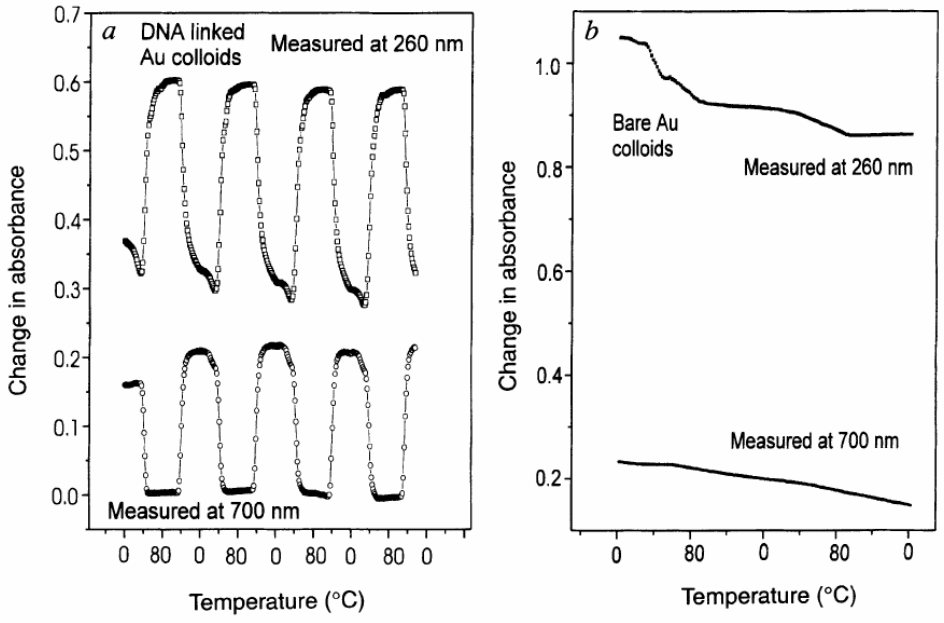

Nature, 1996, 382, 607

Selective Colorimetric Detection of Polynucleotides Based on the Distance-Dependent Optical Properties of Gold Nanoparticles

Robert Elghanian, James J. Storhoff, Robert C. Mucic,
Robert L. Letsinger,* Chad A. Mirkin*

SCIENCE • VOL. 277 • 22 AUGUST 1997

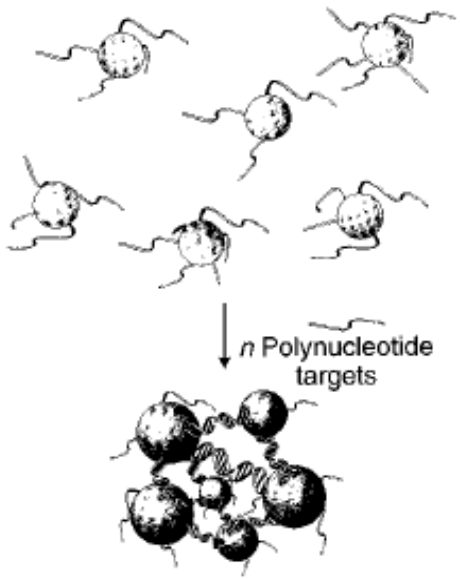

Fig. 1. Schematic representation of the concept for generating aggregates signaling hybridization of nanoparticle-oligonucleotide conjugates with oligonucleotide target molecules. The nanoparticles and the oligonucleotide interconnects are not drawn to scale, and the number of oligomers per particle is believed to be much larger than depicted.

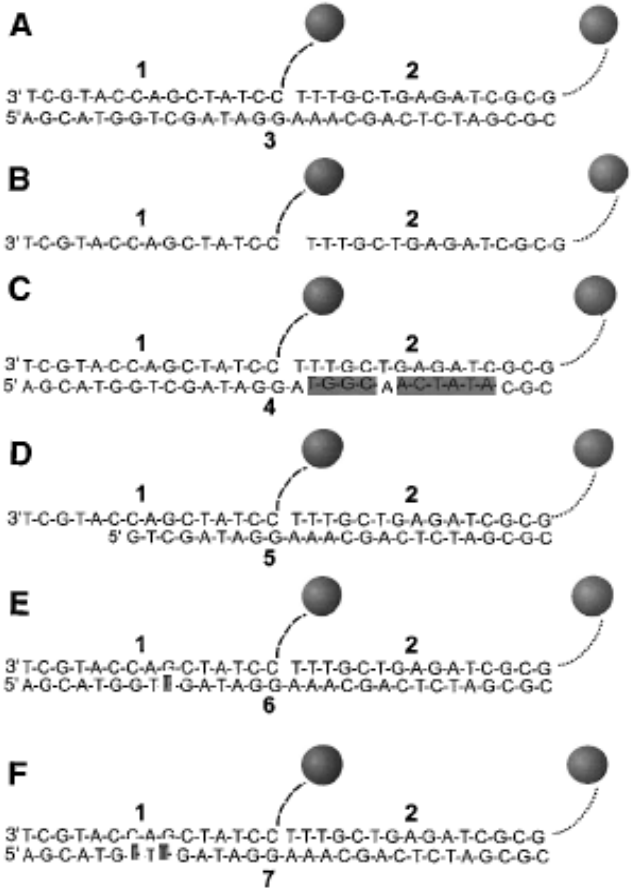

Fig. 2. Mercaptoalkyloligonucleotide-modified 13-nm Au particles and polynucleotide targets used for examining the selectivity of the nanoparticle-based colorimetric polynucleotide detection system. (**A**) Complementary target; (**B**) probes without the target; (**C**) a half-complementary target; (**D**) a 6-bp deletion; (**E**) a 1-bp mismatch; and (**F**) a 2-bp mismatch. For the sake of clarity, only two particles are shown; in reality a polymeric aggregate with many particles is formed. Dashed lines represent flexible spacer portions of the mercaptoalkyloligonucleotide strands bound to the nanoparticles; note that these spacers, because of their noncomplementary nature, do not participate in hybridization. The full sequences for the two probes, **1** and **2**, which bind to targets **3** through **7**, are

1-5′SH-$(CH_2)_6$- [CTA-ATC-CGC-ACA-G]
spacer

[CC-TAT-CGA-CCA-TGC-T]
probe

2-5′SH-$(CH_2)_6$-[ATG-GCA-ACT-ATA-C]
spacer

[GC-GCT-AGA-GTC-GTT-T]
probe

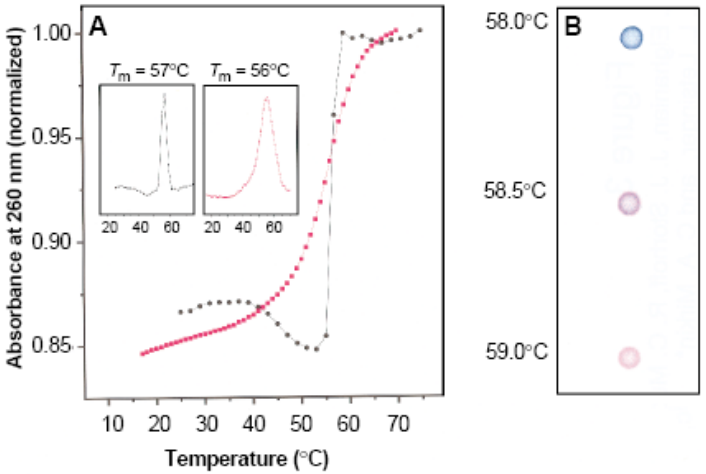

Fig. 3. (**A**) Comparison of the thermal dissociation curves for complexes of mercaptoalkyloligonucleotide-modified Au nanoparticles (black circles) and mercaptoalkyloligonucleotides without Au nanoparticles (red squares) with the complementary target, **3**, in hybridization buffer (0.1 M NaCl, 10 mM phosphate buffer, pH 7.0). For the first set (black circles), a mixture of 150 μl of each colloid conjugate and 3 μl of the target oligonucleotide in hybridization buffer (0.1 M NaCl, 10 mM phosphate, pH 7.0) was frozen at the temperature of dry ice, kept for 5 min, thawed over a period of 15 min, and diluted to 1.0 ml with buffer (final target concentration, 0.02 μM). The absorbance was measured at 1-min intervals with a temperature increase of 1°C per minute. The increase in absorption at 260 nm (A_{260}) was ~0.3 absorption units (AU). In the absence of the oligonucleotide targets, the absorbance of the nanoparticles did not increase with increasing temperature. For the second set, the mercaptoalkyloligonucleotides and complementary target (each 0.33 μM) were equilibrated at room temperature in 1 ml of buffer, and the changes in absorbance with temperature were monitored as before. The increase in A_{260} was 0.08 AU. (**Insets**) Derivative curves for each set (*15*). (**B**) Spot test showing T_c (thermal transition associated with the color change) for the Au nanoparticle probes hybridized with complementary target. A solution prepared from 150 μl of each probe and 3 μl of the target (0.06 μM final target concentration) was frozen for 5 min, allowed to thaw for 10 min, transferred to a 1-ml cuvette, and warmed at 58°C for 5 min in the thermally regulated cuvette chamber of the spectrophotometer. Samples (3 μl) were transferred to a C_{18} reverse phase plate with an Eppendorf pipette as the temperature of the solution was increased incrementally 0.5°C at 5-min intervals.

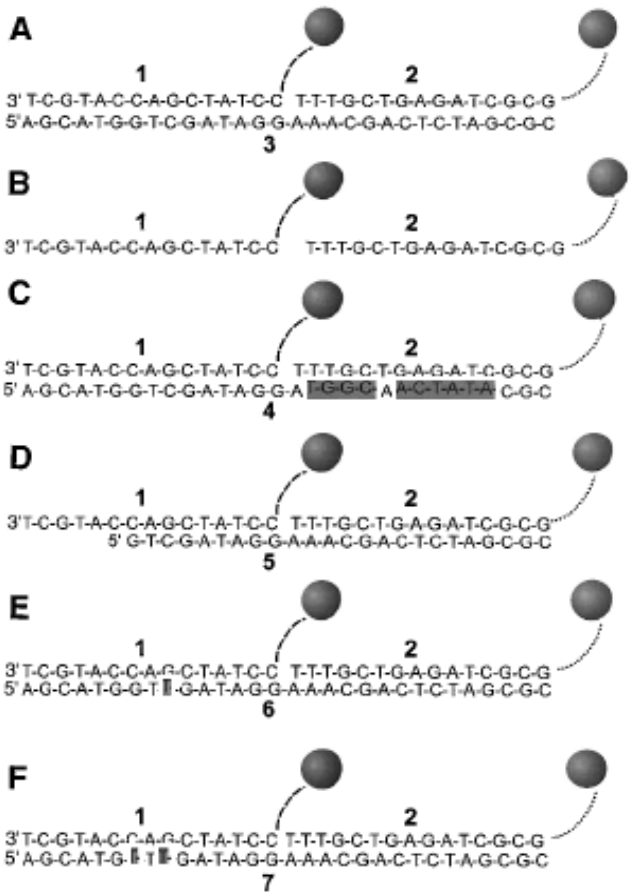

A=T

C=G

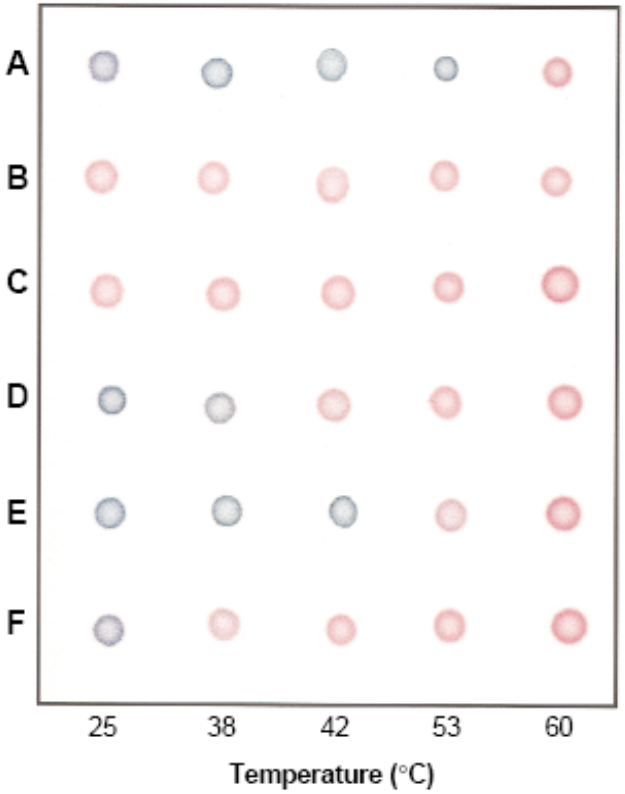

Fig. 4. Selective polynucleotide detection for the target probes shown in Fig. 2: (**A**) complementary target; (**B**) no target; (**C**) complementary to one probe; (**D**) a 6-bp deletion; (**E**) a 1-bp mismatch; and (**F**) a 2-bp mismatch. Nanoparticle aggregates were prepared in a 600-μl thin-walled Eppendorf tube by addition of 1 μl of a 6.6 μM oligonucleotide target to a mixture containing 50 μl of each probe (0.06 μM final target concentration). The mixture was frozen (5 min) in a bath of dry ice and isopropyl alcohol and allowed to warm to room temperature. Samples were then transferred to a temperature-controlled water bath, and 3-μl aliquots were removed at the indicated temperatures and spotted on a C_{18} reverse phase plate.

J. Am. Chem. Soc. **1998,** *120,* 1959−1964

One-Pot Colorimetric Differentiation of Polynucleotides with Single Base Imperfections Using Gold Nanoparticle Probes

James J. Storhoff, Robert Elghanian, Robert C. Mucic, Chad A. Mirkin,* and Robert L. Letsinger*

Scheme 1

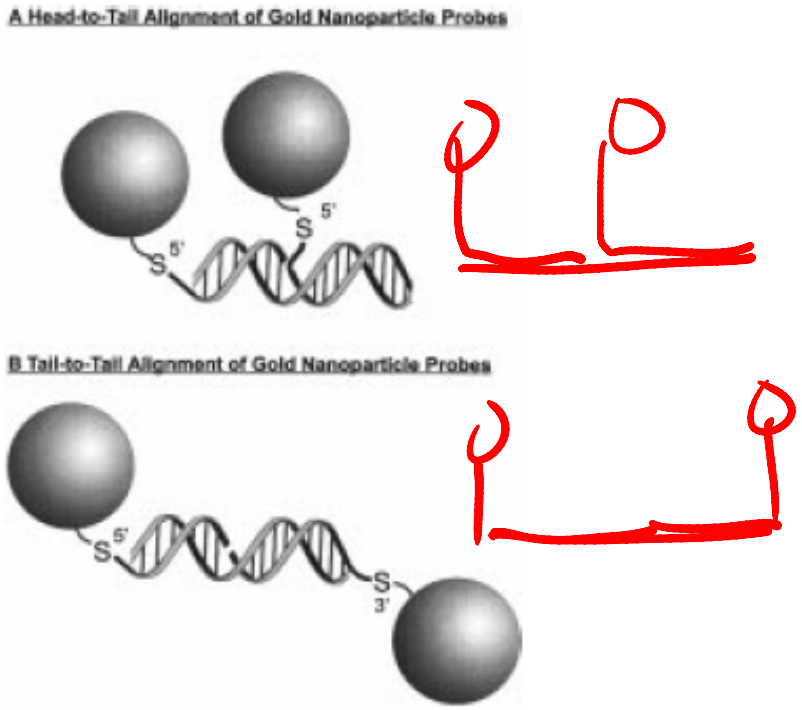

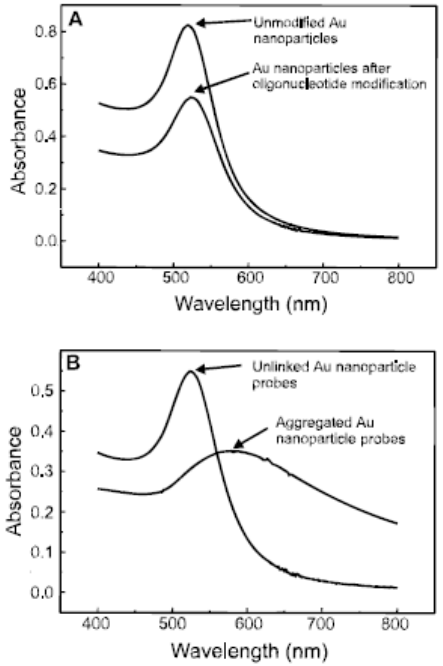

Figure 1. (A) Comparison of UV−vis spectra for 300 mL of ~13 nm diameter Au nanoparticles in 1 mL total of aqueous solution and 300 mL of ~13 nm diameter gold nanoparticles functionalized with 5′-hexanethiol 12-base oligonucleotides in 1 mL total of 0.3 M NaCl, 10 mM phosphate (pH 7) solution. (B) Comparison of Au nanoparticles functionalized with 5′-hexanethiol 12-base oligonucleotides (**1** and **2**, see Figure 2A) before and after treatment with a complementary 24-base oligonucleotide (see the Experimental Section under Melting Analyses for preparation procedure of the aggregate solution).

Tail-to Tail

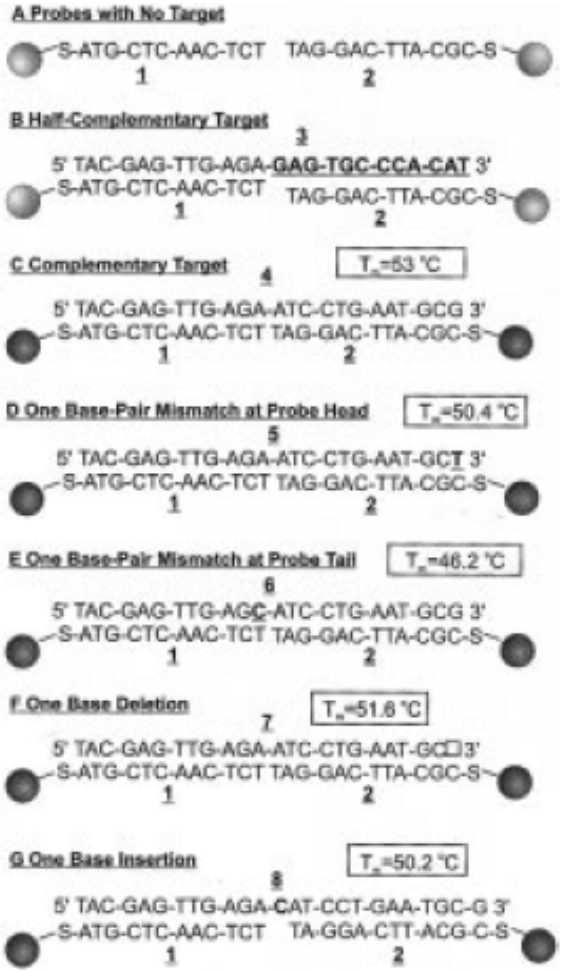

Figure 2. (Alkanethiol)oligonucleotide-modified 13 nm diameter Au nanoparticle probes (**1** and **2**) and polynucleotide target sequences (**3**–**8**) used for examining the selectivity of the nanoparticle-based colorimetric polynucleotide detection system. Portions of the target sequences which are underlined in bold represent mismatched bases, bold lettering represents an inserted base, and a box represents a deletion in the polynucleotide. The "melting temperatures" of the Au nanoparticle/target polynucleotide aggregate structures are shown in boxes. Only one attached oligonucleotide is shown per particle even though each particle actually has many oligonucleotides attached to it. Also, only two particles are shown aligning on a target strand; in reality, large extended networks of Au nanoparticles are formed.

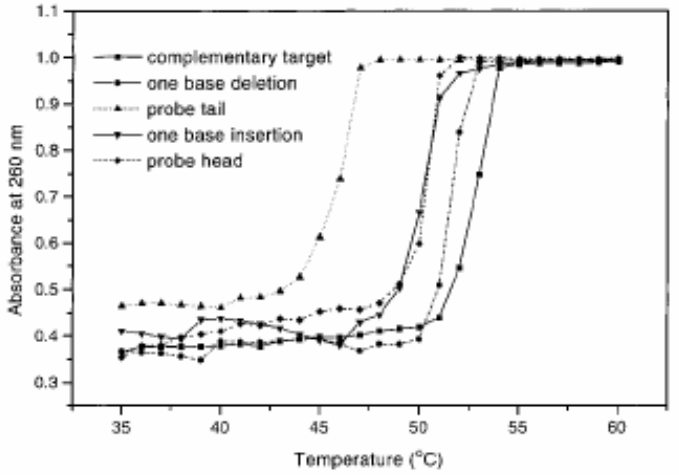

Figure 3. Comparison of the normalized thermal dissociation curves for Au nanoparticle probes (**1** and **2**) with a fully complementary target (**4**) and targets containing single base imperfections (**5**–**8**) in hybridization buffer (0.3 M NaCl, 10 mM phosphate (pH 7)), see Figure 2 for sequences and T_m values. Absorbance values at 260 nm were recorded at 1 °C intervals with a holding time of 1 min/deg from 25 to 75 °C. Here, only the region from 35 to 60 °C is shown.

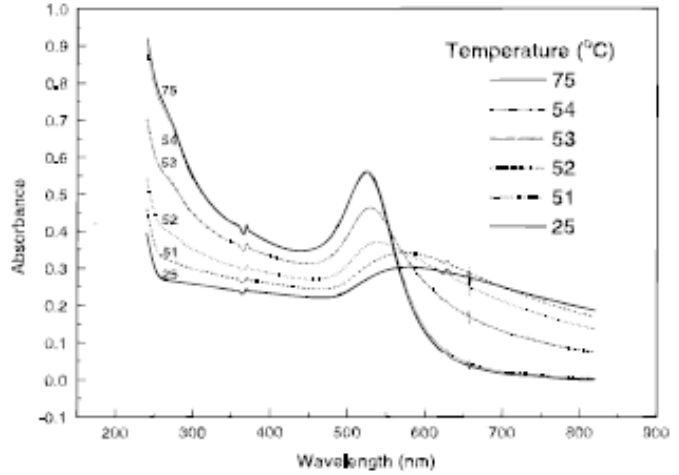

Figure 4. UV–vis spectra from the melting analysis of the Au nanoparticle probe/target polynucleotide aggregate solution which show the spectral changes associated with thermal dissociation of the aggregate. Here, only selected temperatures which illustrate the major changes in aggregate dissociation are shown (25, 51, 52, 53, 54, 75 °C).

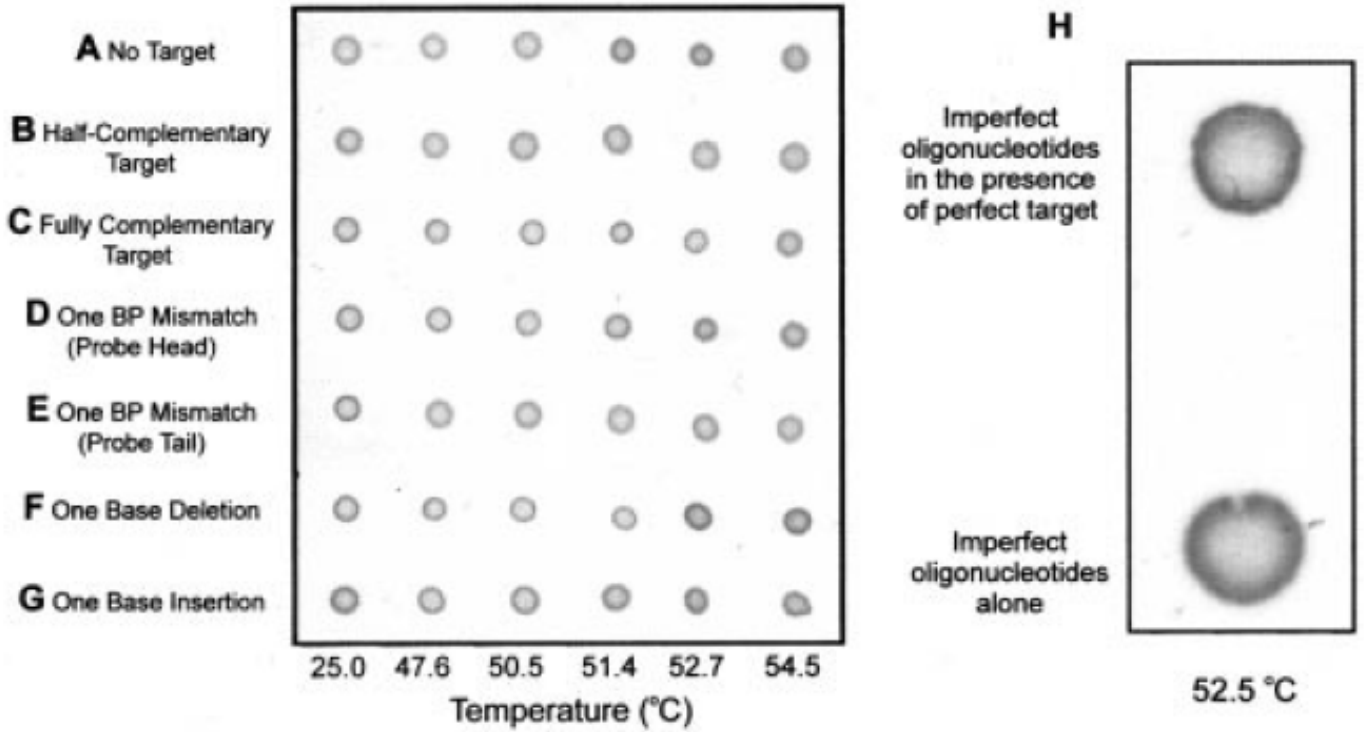

Figure 5. (A–G) The spot method for polynucleotide detection which demonstrates the selectivity of the Au nanoparticle based detection system toward single base imperfections. The probes and corresponding polynucleotide targets are listed in Figure 2. (H) Spot test demonstrating the detection and differentiation by color of a polynucleotide target in the presence of polynucleotides with single base imperfections.

1nM => 50pM

Rapid Aggregation of Gold Nanoparticles Induced by Non-Cross-Linking DNA Hybridization

Kae Sato, Kazuo Hosokawa, and Mizuo Maeda*

8102 ■ J. AM. CHEM. SOC. 2003, *125*, 8102−8103

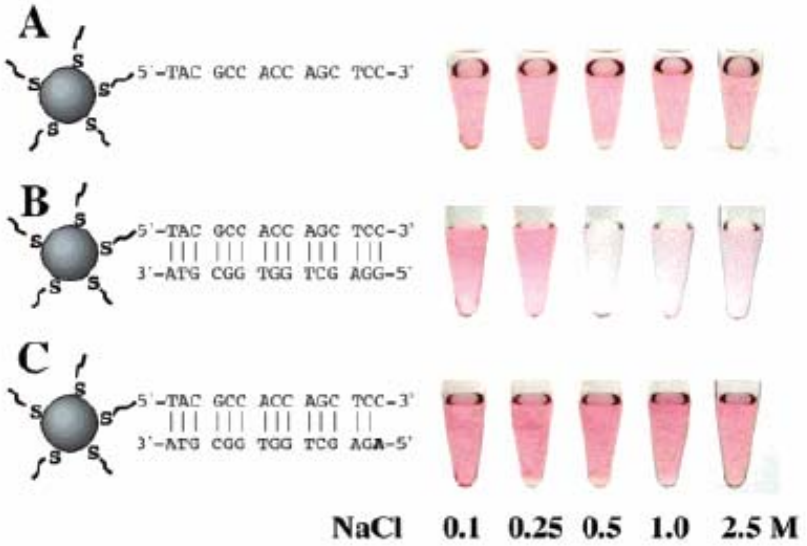

Figure 1. Aggregation behaviors of the DNA-gold nanoparticles at various NaCl concentrations at room temperature: (A) without a target DNA, (B) with the complementary target, and (C) with a target containing a single-base mismatch at its 5′ terminus. The final concentrations of the particle, the probe DNA, and the targets were 2.3, 500, and 500 nM, respectively.

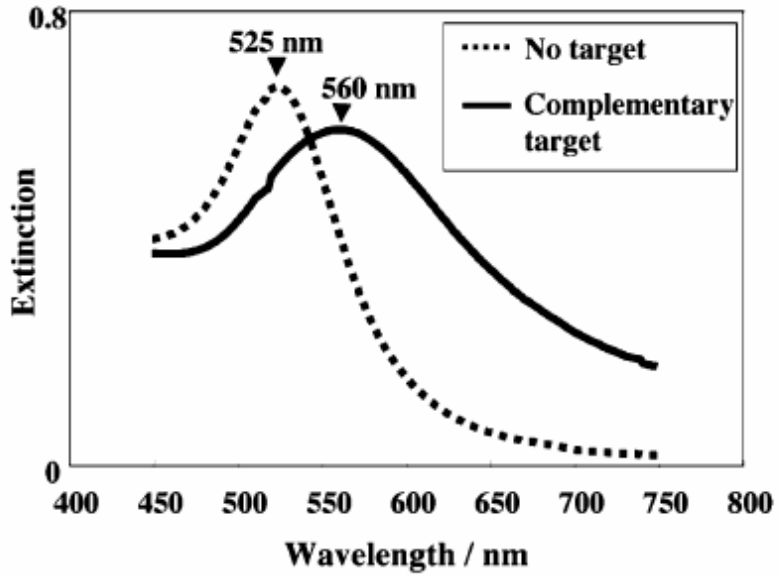

Figure 2. Visible spectra corresponding to Figure 1A (dotted line, no target) and 1B (solid line, complementary target) at 0.5 M NaCl.

60-500 nM

Label-Free Colorimetric Detection of Specific Sequences in Genomic DNA Amplified by the Polymerase Chain Reaction

Huixiang Li† and Lewis J. Rothberg*,†,‡

10958 ■ J. AM. CHEM. SOC. 2004, *126*, 10958−10961

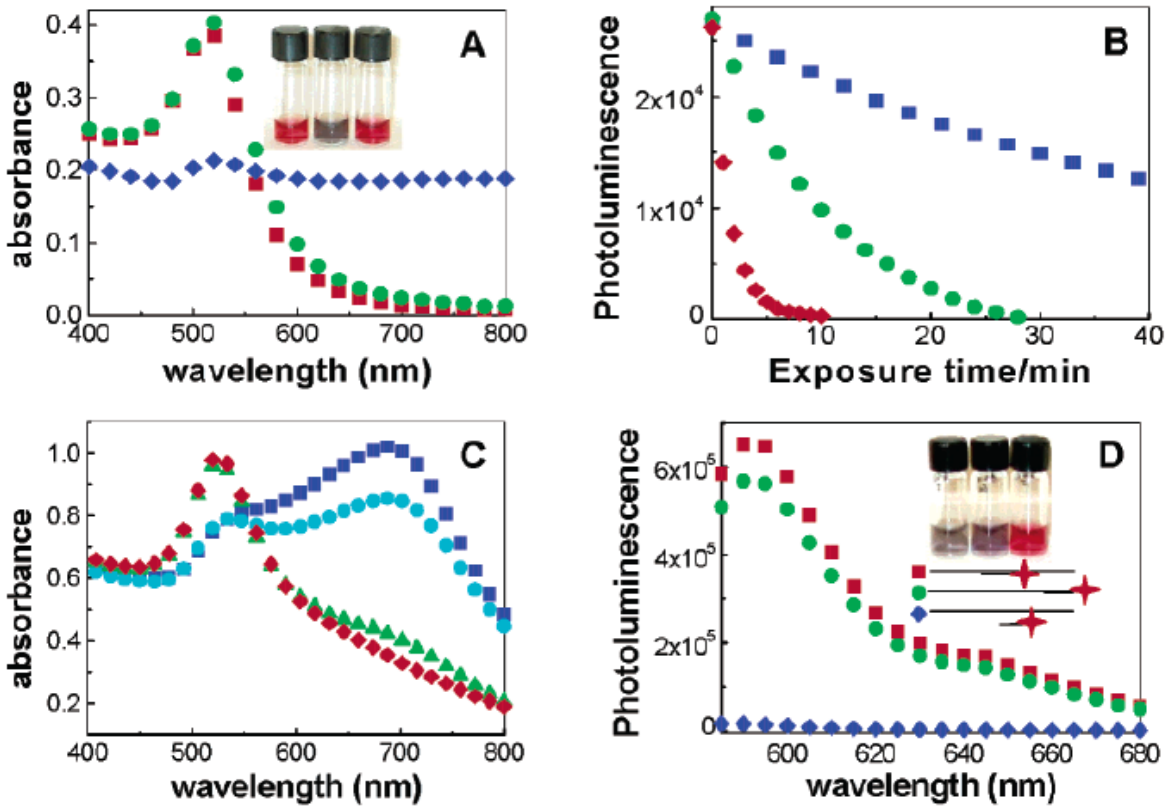

Figure 1. Adsorption of ss-DNA to gold nanoparticles. (A) Absorption spectra of 300 μL of gold colloid and 100 μL of deionized water (red), 100 μL of 10 mM PBS (0.2 M NaCl) (blue), 300 pmol of 24-base ss-DNA first, then 100 μL of 10 mM PBS (0.2 M NaCl) (green). (B) Photoluminescence intensity versus time following the addition of 4 pmol of rhodamine red-tagged ss-DNAs to 1000 μL of gold colloid. 10 mer (red), 24 mer (green), and 50 mer (blue). (C) Absorption spectra of the mixture of 200 pmol of ss-DNA (50 mer) and 300 μL of gold nanoparticles heated at different temperature for 2 min, followed by the addition of 300 μL of 10 mM PBS (0.2 M NaCl). 22 °C (blue), 45 °C (cyan), 70 °C (green), and 95 °C (red). (D) The fluorescence spectra of the hybridized solutions of rhodamine red-labeled 15 mer ss-DNA and 50 mer ss-DNA and gold colloid, the 15 mer binding to the 50 mer in the middle (red), at the end (green) and not at all (blue). The lower inset schematically illustrates the binding positions between the 15 mer and 50 mer. The upper inset contains color photographs of the corresponding mixtures (from left to right) with no fluorescent label on the 15 mer. See the Supporting Information for experimental details.

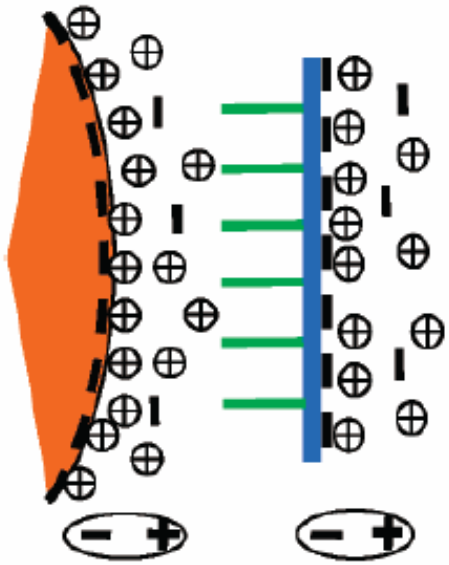

Figure 2. Schematic of the interaction between negatively charged Au-np and ss-DNA. The orange wedge represents the Au-np, the green lines represent the DNA bases, and the blue line represents the phosphate backbone.

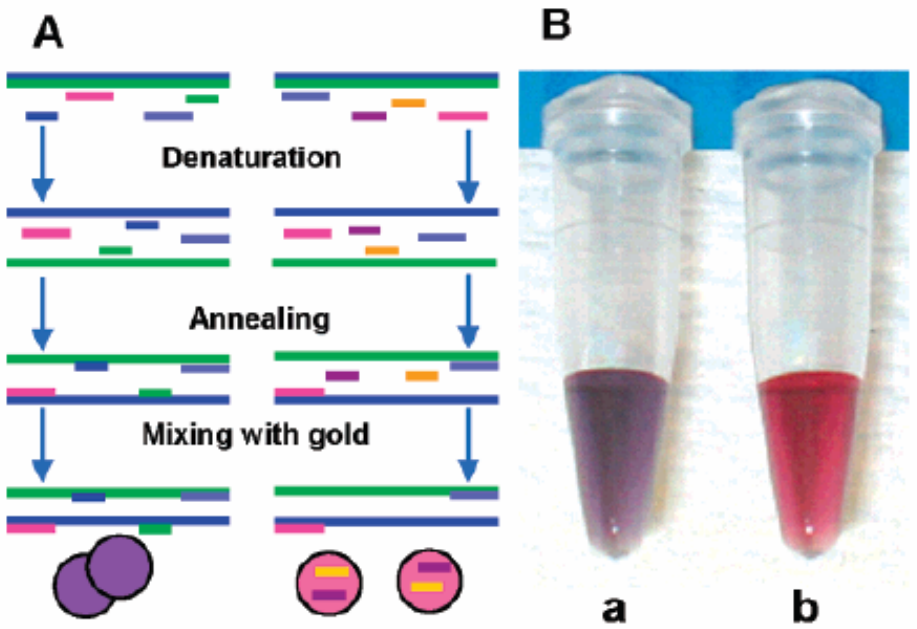

Figure 3. Identification of PCR-amplified DNA sequences. (A) Schematic of the detection protocol. The mixture of PCR product and probes is denatured and annealed below the melting temperature of the complementary probes followed by addition of gold colloid. The long blue and green lines represent the PCR-amplified DNA fragments, and the pink and light blue medium bars represent the excess PCR primers. The short blue and green bars are complementary probes that bind, resulting in Au-np aggregation (purple color). The short purple and orange bars are noncomplementary probes that do not bind and adsorb to the Au-np, preventing Au-np aggregation and leaving the solution pink. (B) Color photographs of the resulting solutions with complementary probes (a) and noncomplementary probes (b). We used 8 μL of PCR product, 3.5 pmol of probe, and 70 μL of gold colloid in each vial.

SNP
One pair mismatch
Lower melting T

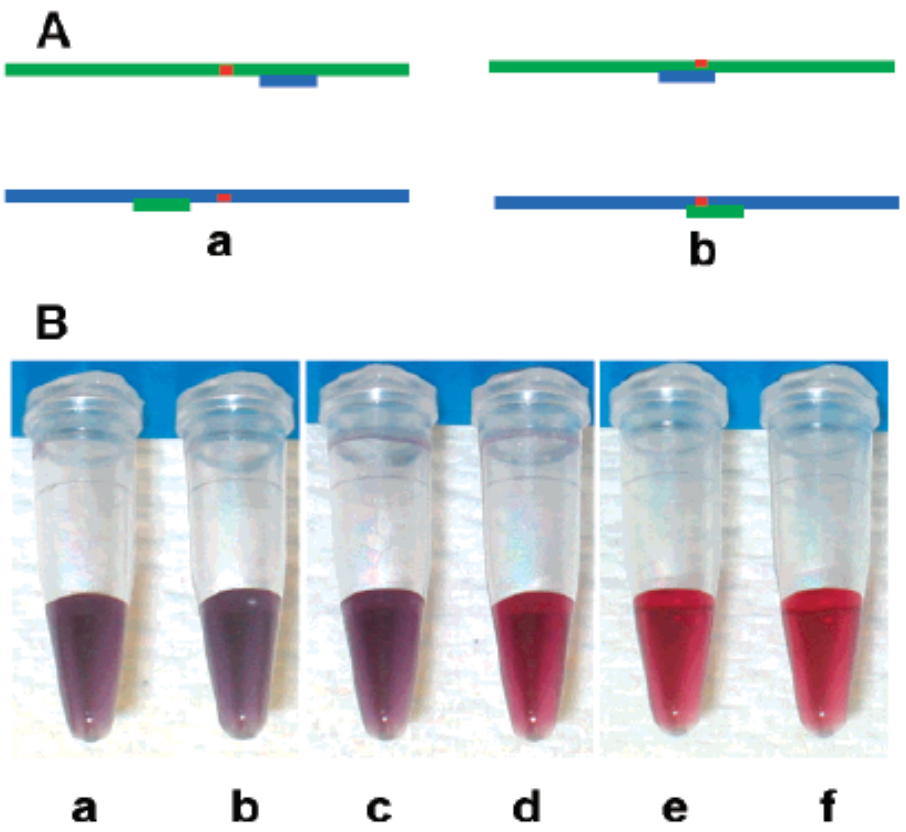

Figure 4. Single base-pair mismatch detection. (A) Detection strategy. The red spots on the long green and blue lines represent positions of a potential SNP. The long green and blue lines are the complementary sequences of the PCR-amplified DNA fragment. The short green and blue bars are probes complementary to parts of the wild-type sequence of the PCR-amplified DNA fragment as illustrated. (B) Detection of a single base-pair mismatch. Vials b, d, and f contain PCR product with probes overlapping the single-base mismatch, while a, c, and e contain PCR product with probes not overlapping the single base-pair mismatch. Photographs are taken of the mixtures annealed at 50 °C (a, b), 54 °C (c, d), and 58 °C (e, f). We used 8 μL of PCR product, 3.5 pmol of probe, and 70 μL of gold colloid in each vial.

J. Am. Chem. Soc. **2000,** *122,* 9071−9077

Colloidal Au-Enhanced Surface Plasmon Resonance for Ultrasensitive Detection of DNA Hybridization

Lin He, Michael D. Musick, Sheila R. Nicewarner, Frank G. Salinas, Stephen J. Benkovic, Michael J. Natan, and Christine D. Keating*

Scheme 1. SPR Surface Assembly

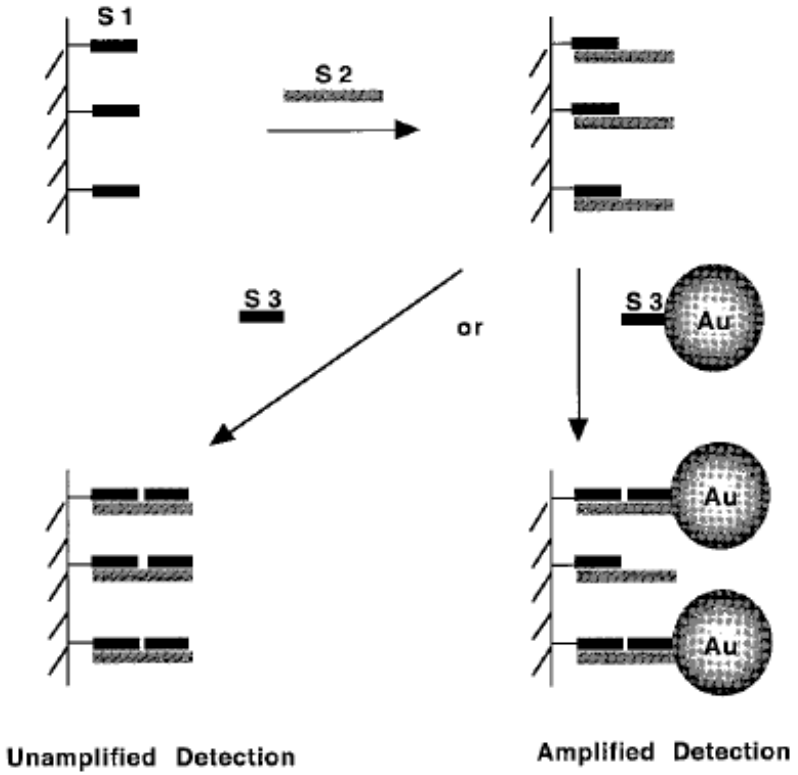

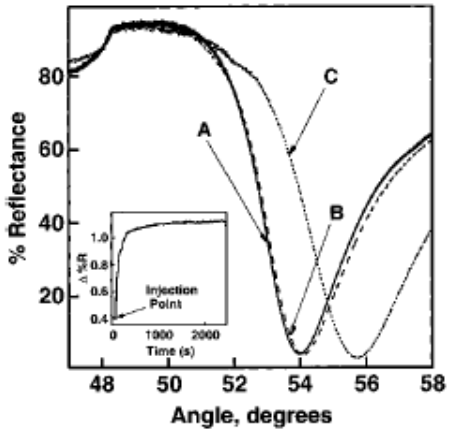

Figure 1. SPR curves of surfaces prepared in sequential steps as illustrated in Scheme 1: a MHA-coated Au film modified with a 12-mer oligonucleotide S1(A), after hybridization with its complementary 24-mer target S2 (B), and followed by introduction of S3:Au conjugate (C) to the surface. Inset: surface plasmon reflectance changes at 53.2° for the oligonucleotide-coated Au film measured during a 60-min exposure to S3:Au conjugates.

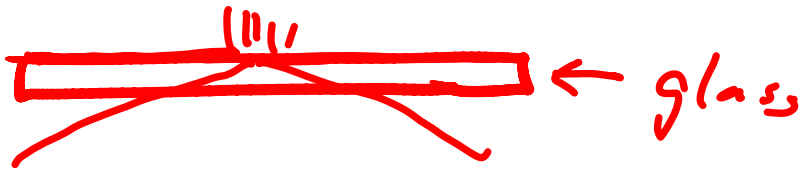

Scheme 2. SPR Surface Assembly in the Digestion Experiment

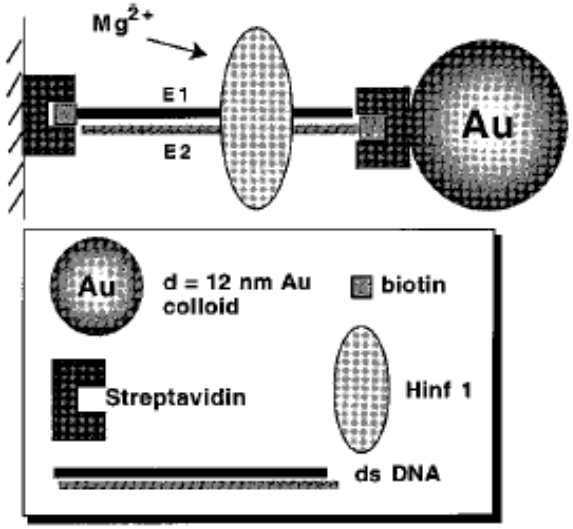

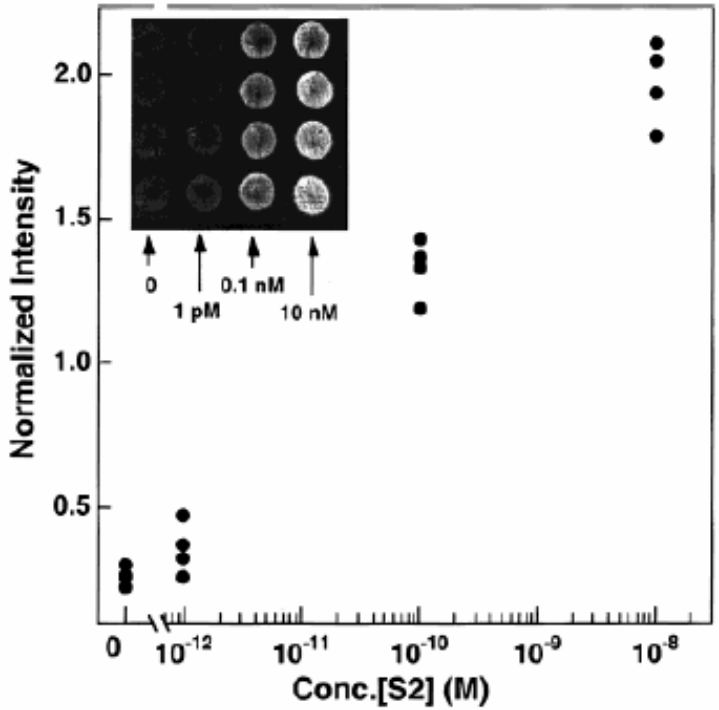

Figure 5. Plot of normalized intensity of SPR reflectance as a function of logarithmic concentration of the analyte 24-mer oligo (S2). Each spot represents one data point at the corresponding concentration. CCD parameters: exposure time = 0.3 s, 16 bit resolution, spot size = 4.5 mm in diameter. Inset: a 2-D SPR image of a Au surface derivatized with 20 μL of buffer blank, 1 pM, 0.1 nM, and 10 nM S2 oligos (from left to right, respectively).

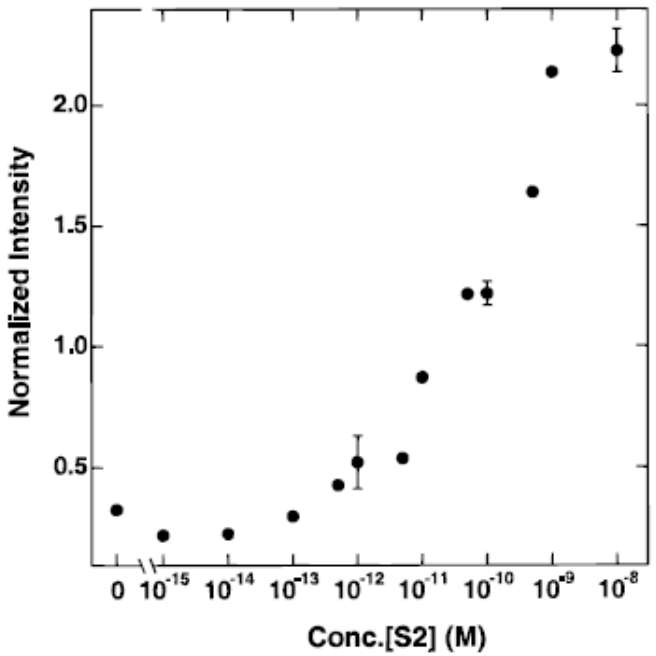

Figure 7. Plot of normalized intensity of SPR reflectance as a function of logarithmic concentration of the analyte 24-mer oligo (S2) from the image shown in Figure 6. The error bars are standard deviations from the data in Figure 5.

Table 1. Comparison of Sensitivity for Au−Amplified SPR in DNA Analysis with Other Techniques

detection method	detection limit of target DNA	refs
radiolabeling	100 fg	71
fluorescence	1.2×10^7 probes/cm^2	36
unamplified scanning SPR	100 fg/100 μm^2 for 10-mer oligos, 150 nM ~120 bp DNA	33, 35
unamplified imaging SPR	10 nM 16-mer oligos	63
Au-amplified scanning SPR	lower than 10 pM 24-mer oligos[a]	this work
Au-amplified imaging SPR	10 pM 24-mer oligos, ≤12 pg/cm^2 (≤8×10^8 oligonucleotides/cm^2)[b]	this work

[a] The spots on SPR imaging surface can be detected by scanning SPR with ease, which demonstrated a lower detection limit can be achieved with the scanning instrument. Considering an instrumental angle resolution limit of 0.005°, a theoretical detection limit of 2×10^7 particles/cm^2 can be realized.[21] [b] The oligonucleotide surface coverage reported for these experiments is an upper limit, determined by assuming 100% of the molecules in solution hybridized to the surface.

A Gold Nanoparticle Based Approach for Screening Triplex DNA Binders

Min Su Han, Abigail K. R. Lytton-Jean, and Chad A. Mirkin*

4954 ■ J. AM. CHEM. SOC. 2006, *128*, 4954−4955

Scheme 1. Representation of Structure and Color Change of Nanoassembly in the Presence of Triplex Binder at Room Temperature

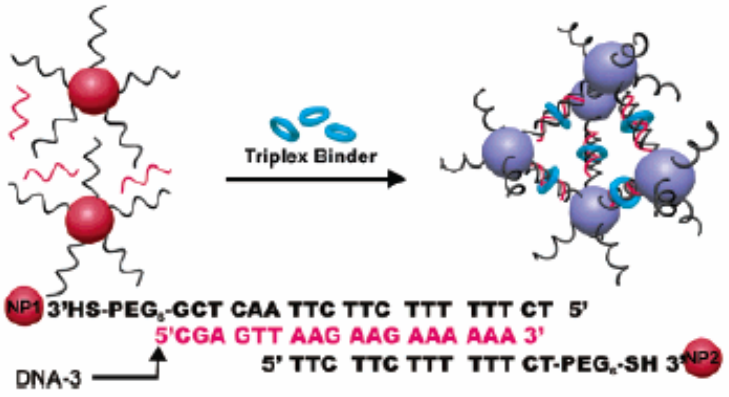

Figure 3. The color change of nanoassembly (NP-1, NP-2, and DNA-3) in the absence and presence of DNA binders at room temperature.

Sequence specific

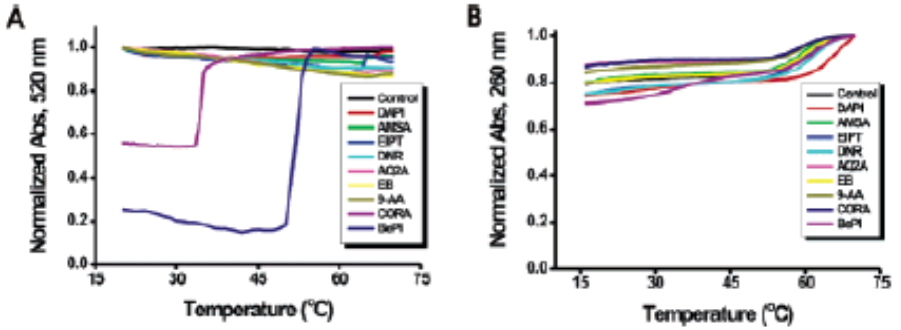

Figure 2. Melting curves of (A) NP-1, NP-2, and DNA-3 assemblies in the presence of DNA binders, (B) DNA-1, DNA-2, and DNA-3 (no nanoparticles) in the presence of DNA binders.

Self-Assembled Nanoparticle Probes for Recognition and Detection of Biomolecules

Dustin J. Maxwell, Jason R. Taylor, and Shuming Nie*,†

9606 ■ J. AM. CHEM. SOC. 2002, *124*, 9606−9612

FRET

D A

D

A

1~10 Å

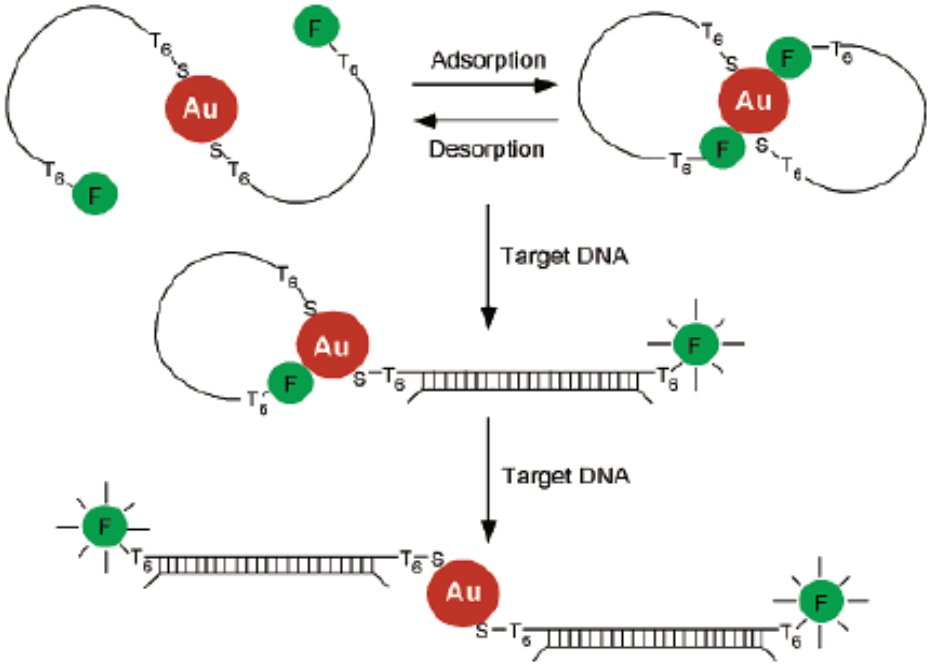

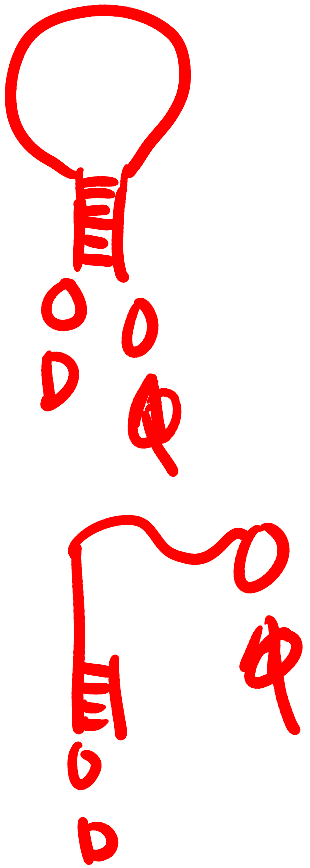

Figure 1. Nanoparticle-based probes and their operating principles. Two oligonucleotide molecules (oligos) are shown to self-assemble into a constrained conformation on each gold particle (2.5 nm diameter). A T_6 spacer (six thymines) is inserted at both the 3′- and 5′-ends to reduce steric hindrance. Single-stranded DNA is represented by a single line and double-stranded DNA by a cross-linked double line. In the assembled (closed) state, the fluorophore is quenched by the nanoparticle. Upon target binding, the constrained conformation opens, the fluorophore leaves the surface because of the structural rigidity of the hybridized DNA (double-stranded), and fluorescence is restored. In the open state, the fluorophore is separated from the particle surface by about 10 nm. See text for detailed explanation. Au, gold particle; F, fluorophore; S, sulfur atom.

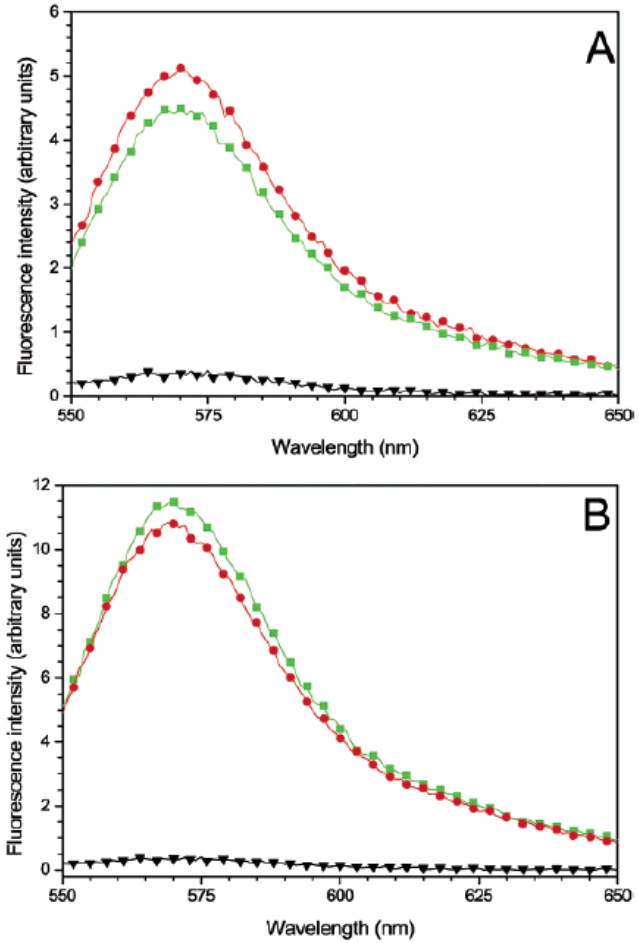

Figure 5. Fluorescence responses and the lack of sequence recognition abilities observed for nonthiolated nanoparticle probes. (A) Fluorescence spectra of nonthiolated probes generated by a complementary target (red curve), a noncomplementary target (green curve), and no target (black curve). These probes are considered nonfunctional because they do not recognize specific DNA sequences. (B) Fluorescence signals obtained from the supernatant solution when the probes were treated with a complementary target (red curve) or a noncomplementary target (green curve). The result revealed that the oligos were released into solution by nonspecific adsorption of the target on the particle surface. With a thiol group, this release was not observed (little or no signal in solution, black curve in B). The nonfunctional probes were prepared in the same way as the functional probes, except that the 3′-end thiol group was deleted. The intensity differences for the red and green curves were within experimental errors and had no particular significance.

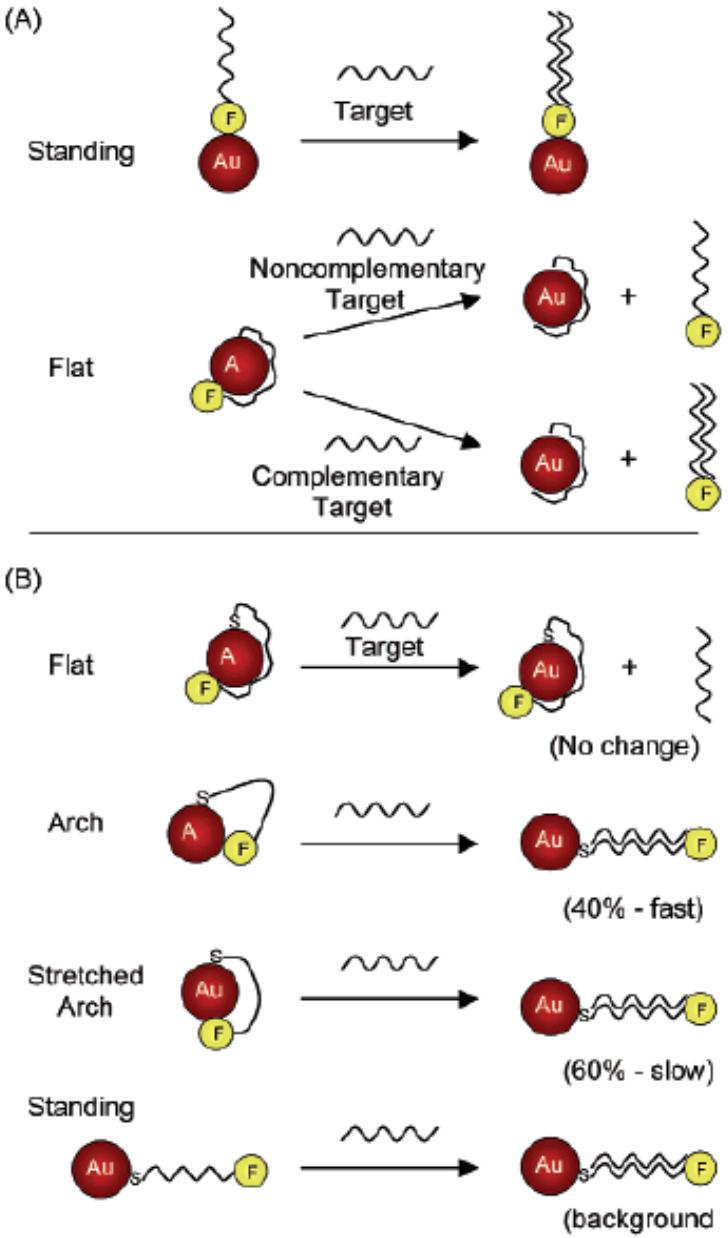

Figure 6. Schematic illustration of possible configurations for (a) nonthiolated and (b) thiolated oligonucleotides adsorbed on colloidal gold nanocrystals. Detailed discussion in text.

Multiplexing by Q-dot

R Red OOGGGG
G
B

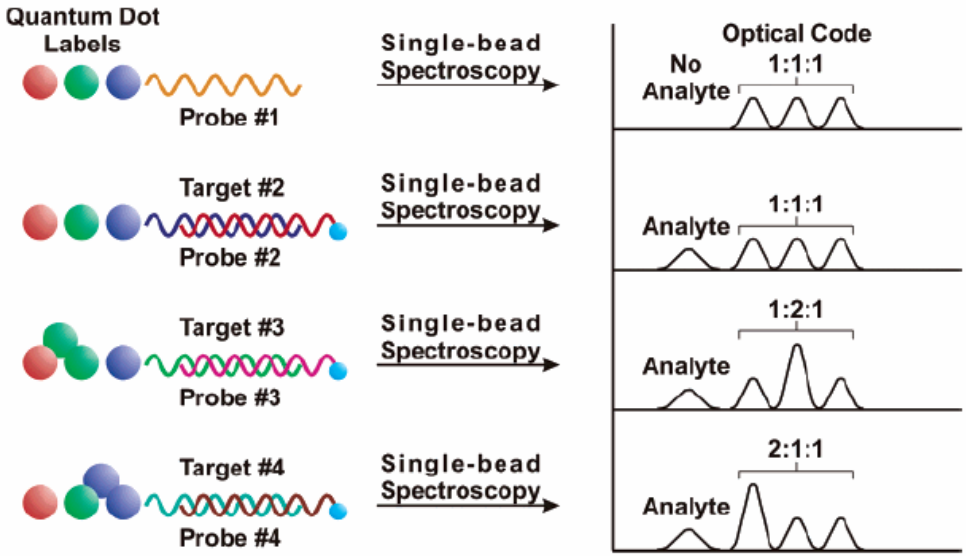

Figure 3. Quantum dots can be employed for detecting multiple targets in a single assay. Specifically, varying the numbers and ratios of different quantum dots per target results in a unique fluorescent signal for each individual target. (Reprinted with permission of Nature Publishing Group. *Nature Biotech.*, Vol. 19, 2001, by Nie, et al.)

Silver Amplification

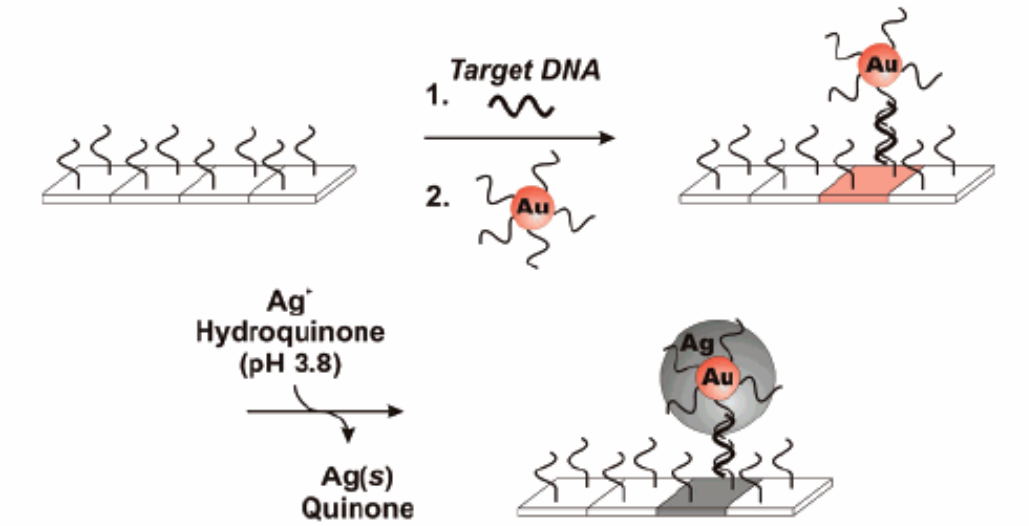

Figure 4. Scanometric DNA assay. In this assay a surface-bound capture oligonucleotide binds one-half of the target of interest, and an oligonucleotide-functionalized gold nanoparticle probe binds to the other half. Catalytic reduction of silver onto the capture/target/probe sandwich results in a signal that can be detected scanometrically. (Reprinted with permission from *Science* (http://www.aaas.org), ref 66. Copyright 2000 American Association for the Advancement of Science.)

Catalytic reduction of Ag on Au

Scanometric DNA Array Detection with Nanoparticle Probes

SCIENCE VOL 289 8 SEPTEMBER 2000

T. Andrew Taton,[1,2] Chad A. Mirkin,[1,2]* Robert L. Letsinger[1]*

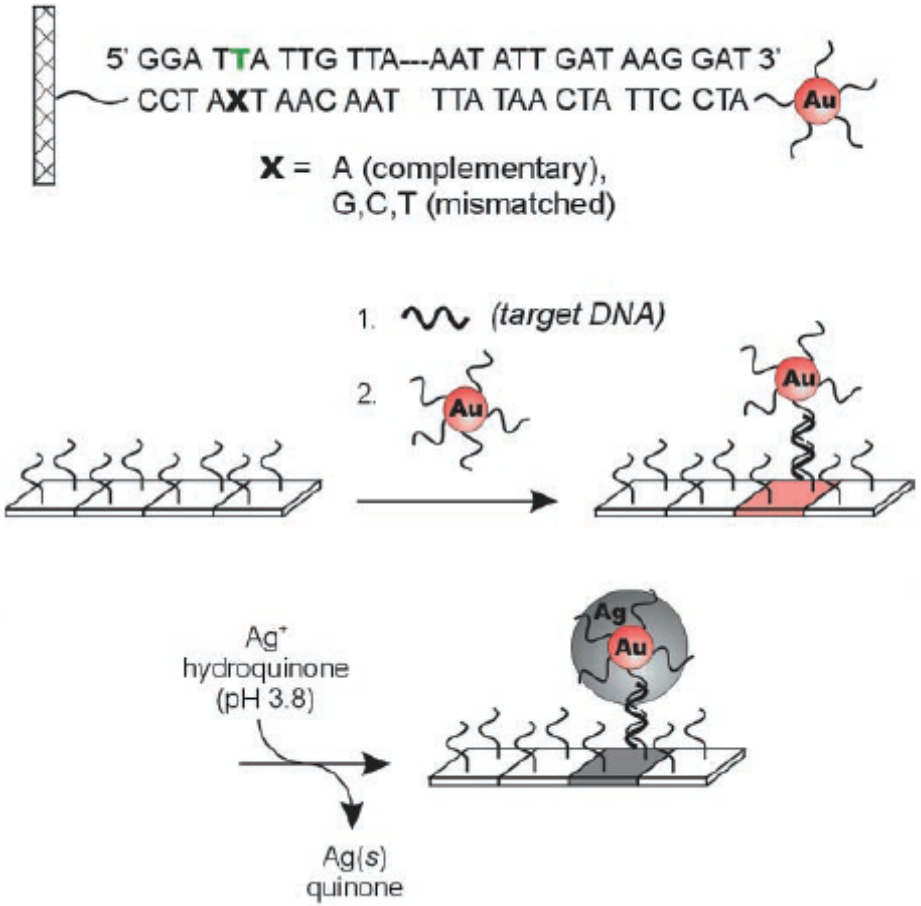

50 fM => 0.2 fM

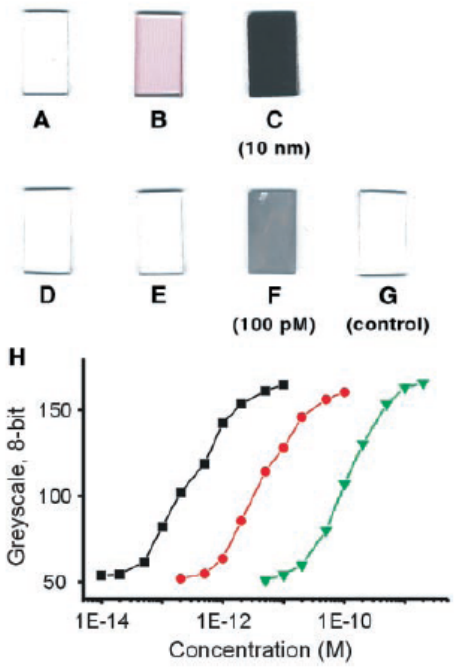

Fig. 1. Images of 7 mm by 13 mm, oligonucleotide-functionalized, float glass slides, obtained with a flatbed scanner. (**A**) Slide before hybridization of target and nanoparticle probe. (**B**) A slide identical to (A) after hybridization with oligonucleotide target (10 nM) and then nanoparticle probes (5 nM in particles). The pink color derives from the Au nanoparticle probes. (**C**) A slide identical to (B) after exposure to silver amplification solution for 5 min. (**D**) Slide before hybridization of target and nanoparticle probe. (**E**) A slide identical to (D) after hybridization with target (100 pM) and then nanoparticle probe (5 nM). The extinction of the submonolayer of nanoparticles is too low to be observed visually or with a flatbed scanner. (**F**) A slide identical to (E) after exposure to silver amplification solution for 5 min. Slide (F) is lighter than slide (C), indicating a lower concentration of target. (**G**) A control slide exposed to 5 nM nanoparticle probe and then exposed to silver amplification solution for 5 min. No darkening of the slide is observed. (**H**) Graph of 8-bit gray scale values as a function of target concentration. The gray scale values were taken from flatbed scanner images of oligonucleotide-functionalized glass surfaces that had been exposed to varying concentrations of oligonucleotide target, labeled with 5 nM oligonucleotide probe and immersed in silver amplification solution. For any given amplification time, the grayscale range is limited by surface saturation at high grayscale values and the sensitivity of the scanner at low values. Therefore, the dynamic range of this system can be adjusted by means of hybridization and amplification conditions (that is, lower target concentrations require longer amplification periods). Squares: 18-base capture-target overlap (*5*), 8× PBS hybridization buffer [1.2 M NaCl and 10 mM NaH_2PO_4/Na_2HPO_4 buffer (pH 7)], 15 min amplification time. Circles: 12-base capture-target overlap, 8× PBS hybridization buffer, 10 min amplification time. Triangles: 12-base capture-target overlap, 2× PBS hybridization buffer [0.3 M NaCl, 10 mM NaH_2PO_4/Na_2HPO_4 buffer (pH 7)], 5 min amplification time. The lowest target concentration that can be effectively distinguished from the background baseline is 50 fM.

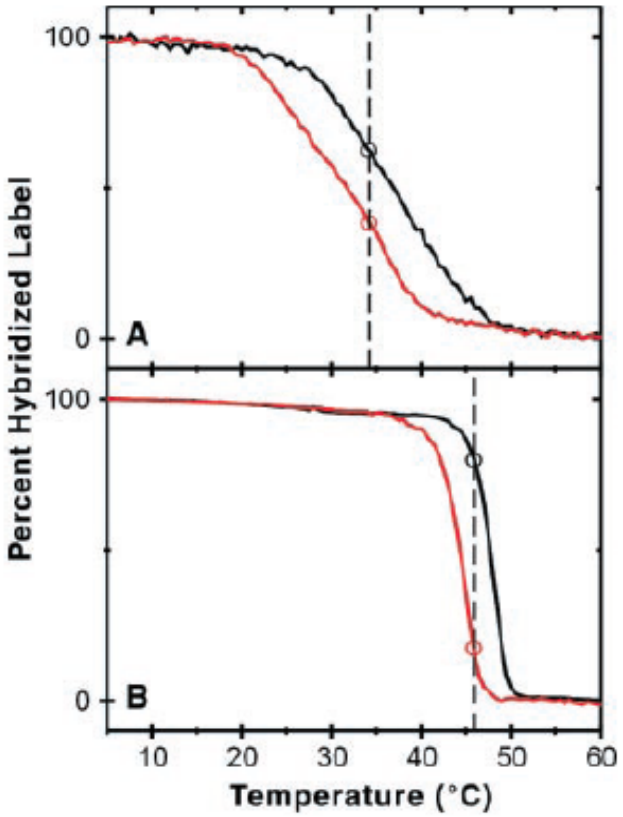

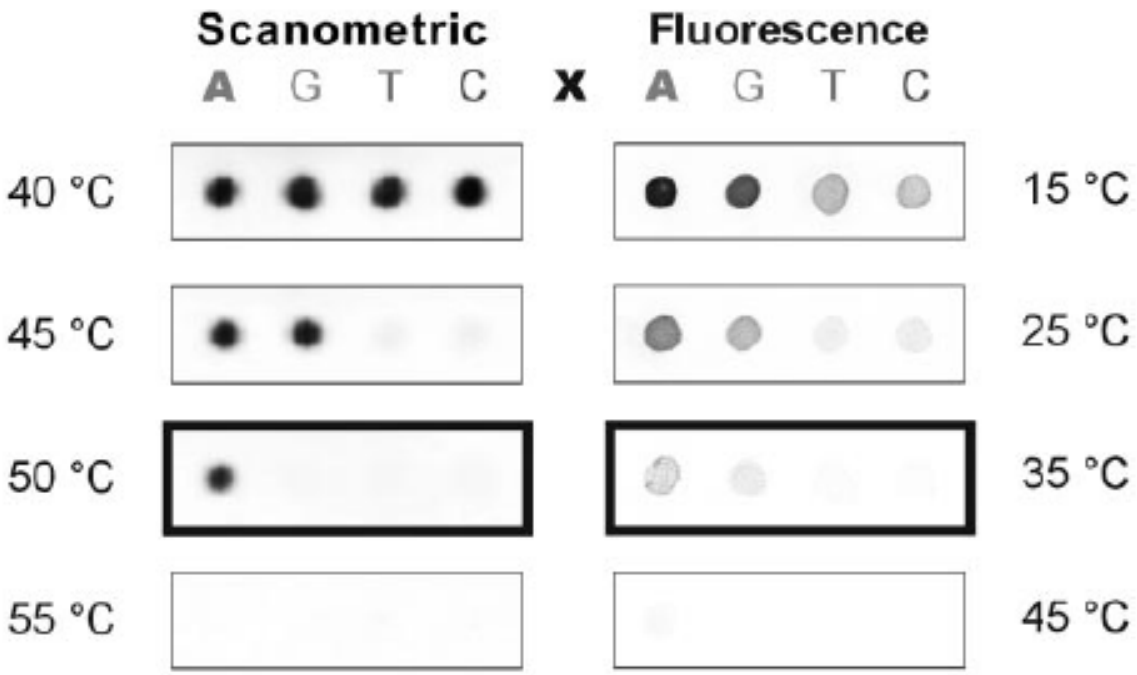

Fig. 3. (**Left**) Nanoparticle-labeled arrays developed at different stringency temperatures. Model oligonucleotide arrays (with the capture sequences shown in Scheme 1) were treated with oligonucleotide target and nanoparticle probes, followed by a 2-min buffer wash at the temperatures shown and subsequent silver amplification (*13*). Images were obtained with an Epson Expression 636 (600 dots per inch) flatbed scanner (Epson America, Long Beach, California). The darkened border indicates the array that showed optimum selectivity for the perfectly complementary target; at this temperature, the ratio of background-subtracted, 8-bit gray scale values for elements A:G:T:C, obtained from histogram averages in Adobe Photoshop (Adobe Systems, San Jose, California), is 96:9:7:6. (**Right**) Fluorophore-labeled arrays washed at different stringency temperatures. Model oligonucleotide arrays identical to those shown at left were treated with oligonucleotide target and Cy3-labeled oligonucleotide probes, followed by a 2-min buffer wash at the temperatures shown. Images were obtained with a ScanArray Confocal Microarray Scanner (GSI Lumonics, Billerica, Massachusetts). The darkened border indicates the array that showed the highest selectivity for the perfectly complementary target, as calculated by the QuantArray Analysis software package (GSI Lumonics); at this temperature, the intensity ratio (in percent, with the intensity of the X = A element at 15°C set to 100%) for elements A:G:T:C is 18:7:1:1.

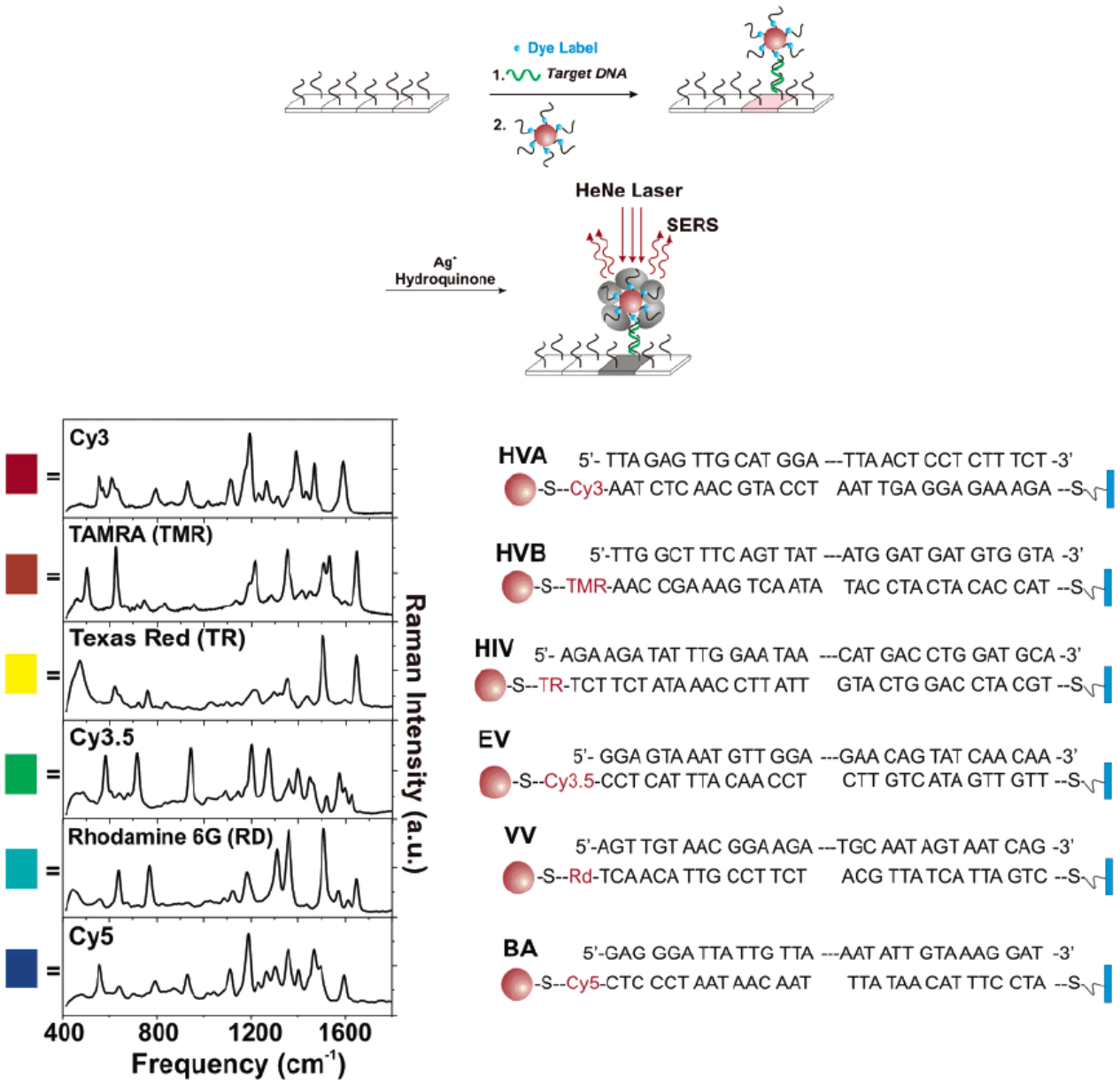

Figure 5. If Raman dyes (blue spheres) are attached to the labeling probe in the scanometric assay, the targets can be encoded and detected via the Raman signal of their labels. (Reprinted with permission from *Science* (http://www.aaas.org), ref 68. Copyright 2002 American Association for the Advancement of Science.)

Nanoparticles with Raman Spectroscopic Fingerprints for DNA and RNA Detection

YunWei Charles Cao, Rongchao Jin, Chad A. Mirkin*

30 AUGUST 2002 VOL 297 SCIENCE

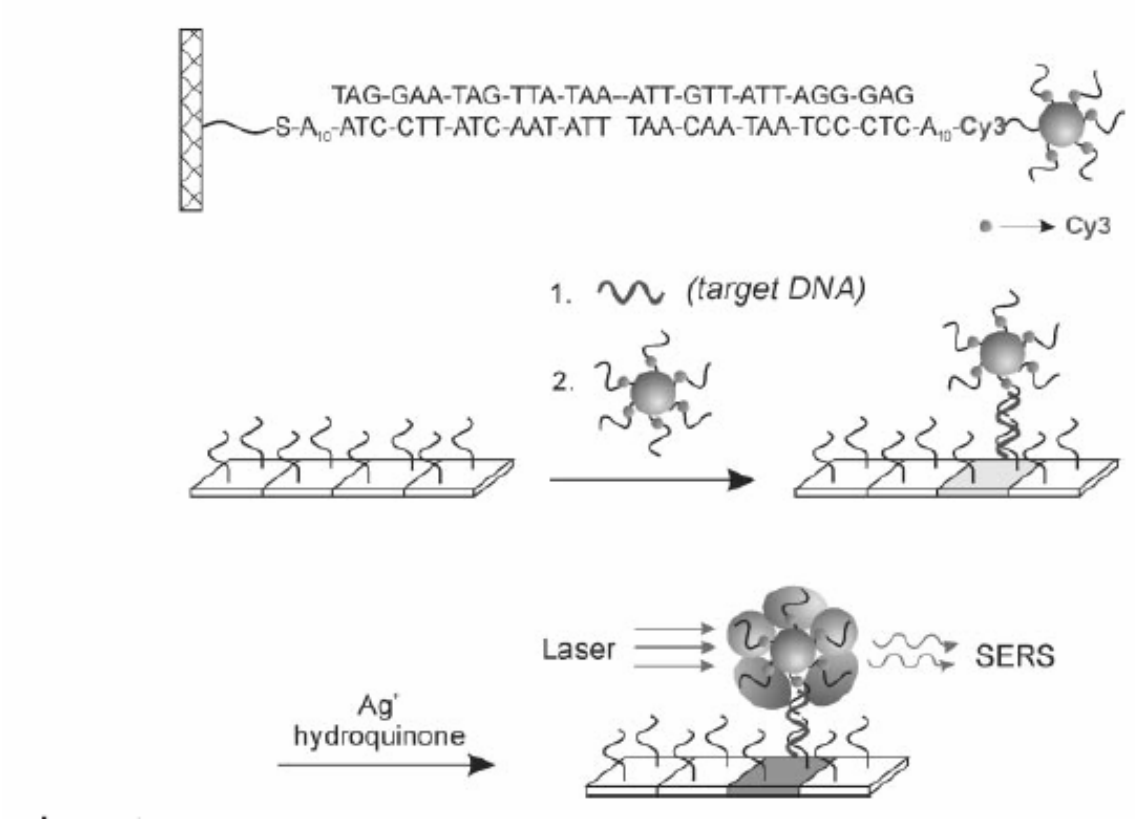

1 fM

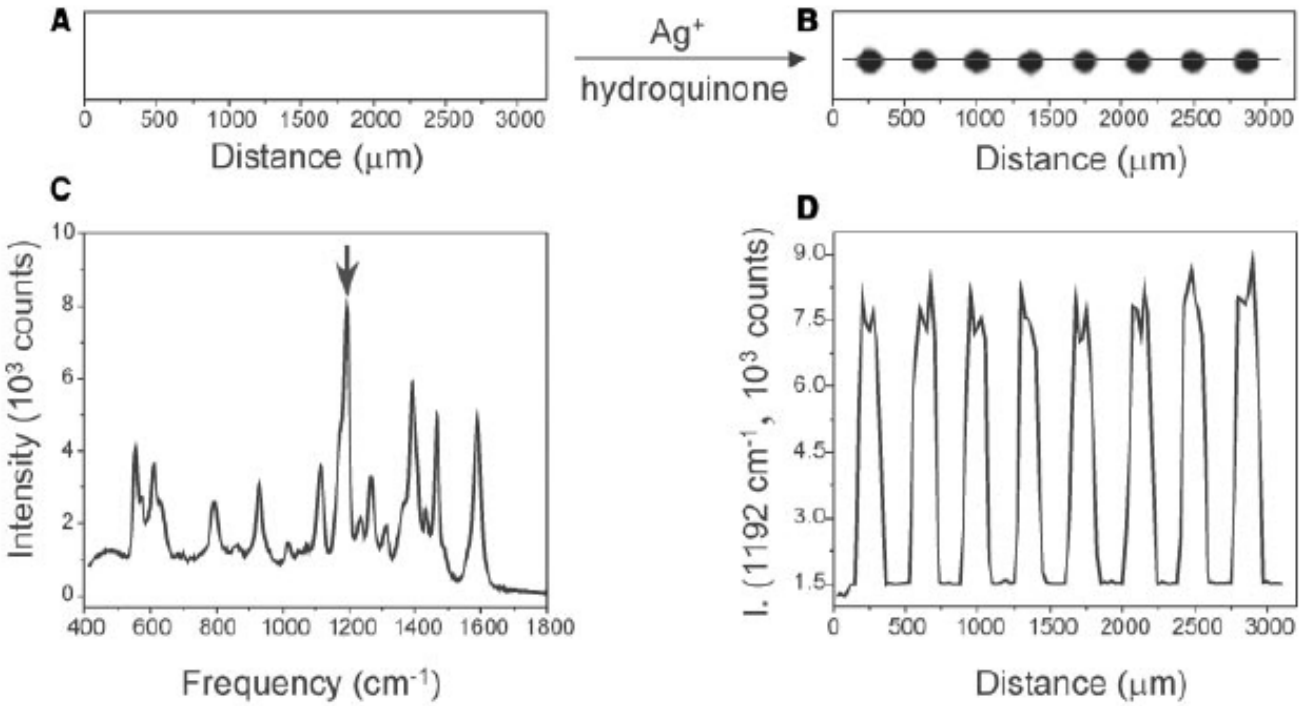

Fig. 1. Flatbed scanner images of microarrays hybridized with nanoparticles (**A**) before and (**B**) after Ag enhancing. (**C**) A typical Raman spectrum acquired from one of the Ag spots. (**D**) A profile of Raman intensity at 1192 cm^{-1} as a function of position on the chip; the laser beam from the Raman instrument is moved over the chip from left to right as defined by the line in (B).

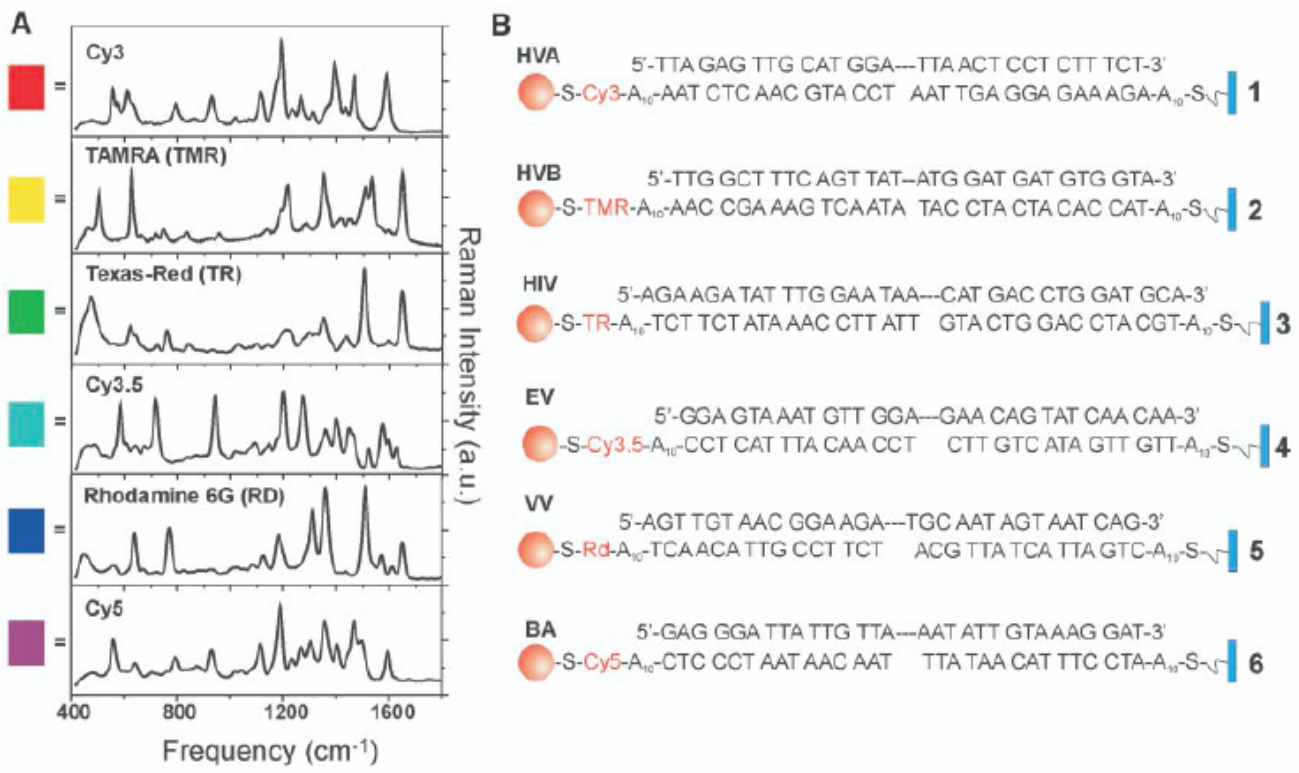

Fig. 2. (**A**) The Raman spectra of six dye-labeled nanoparticle probes after Ag enhancing on a chip (after background subtraction). Each dye correlates with a different color in our labeling scheme (see rectangular boxes). TAMRA, tetramethyl rhodamine. (**B**) Six DNA sandwich assays with corresponding target analysis systems. A_{10} is an oligonucleotide tether with 10 adenosine units.

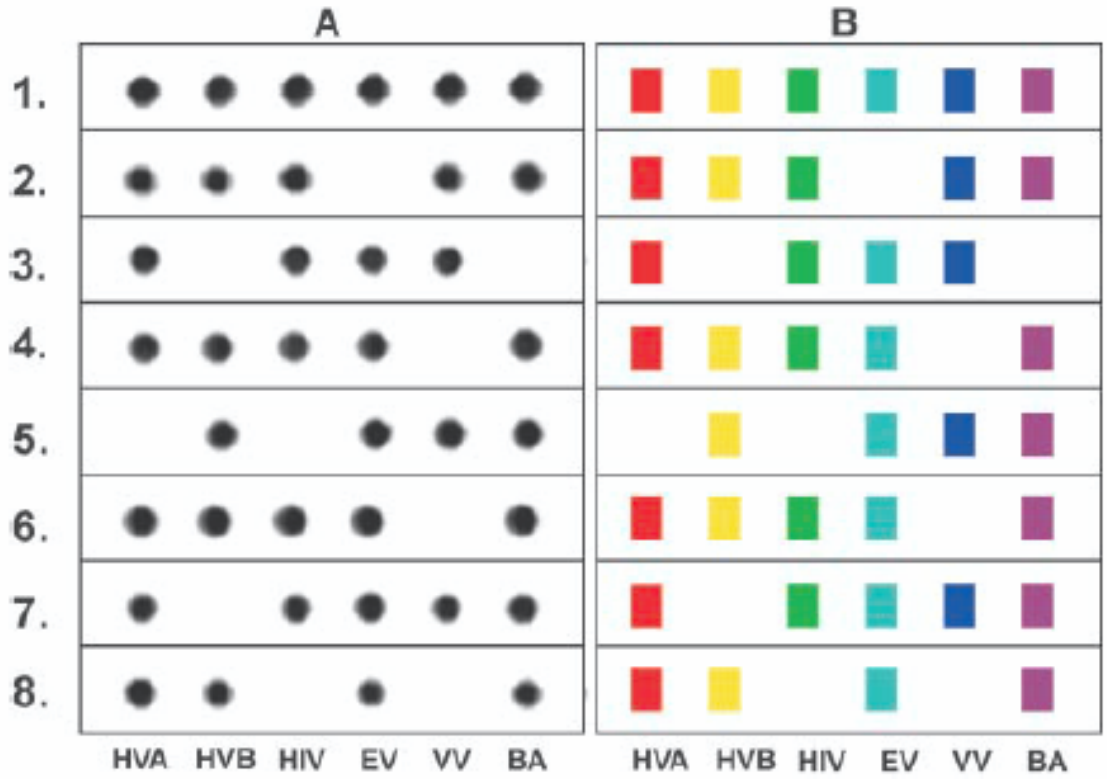

Fig. 3. (**A**) Flatbed scanner images of Ag-enhanced microarrays and (**B**) corresponding Raman spectra. The colored boxes correlate with the color-coded Raman spectra in Fig. 2. No false-positives or false-negatives were observed.

Scheme 2.

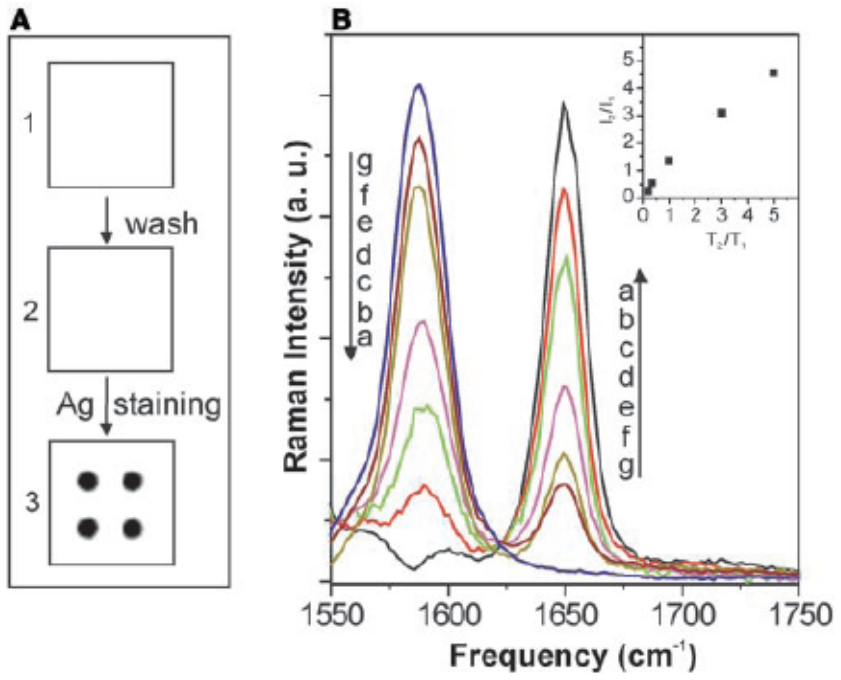

Fig. 4. (**A**) Typical flatbed scanner images of microarrays hybridized with nanoparticles (1) before and (2) after stringency wash but before Ag enhancing, and (3) after Ag enhancing. (**B**) Raman spectra (from 1550 to 1750 cm^{-1}) from the stained spots at different ratios of target 1 and target 2: (a) 1:0; (b) 5:1; (c) 3:1; (d) 1:1; (e) 1:3; (f) 1:5; (g) 0:1. The full Raman spectra from 400 to 1800 cm^{-1} are shown in the supporting text. (Inset) Profile of Raman intensity ratio (I_2/I_1) versus target ratio (T_2/T_1), where I_1 is the Raman intensity at 1650 cm^{-1} (from probe 1, TMR labeled); I_2 is the Raman intensity at 1588 cm^{-1} (from probe 2, Cy3 labeled).

Bio-Bar-Code-Based DNA Detection with PCR-like Sensitivity

Jwa-Min Nam, Savka I. Stoeva, and Chad A. Mirkin*

J. AM. CHEM. SOC. 2004, *126*, 5932−5933

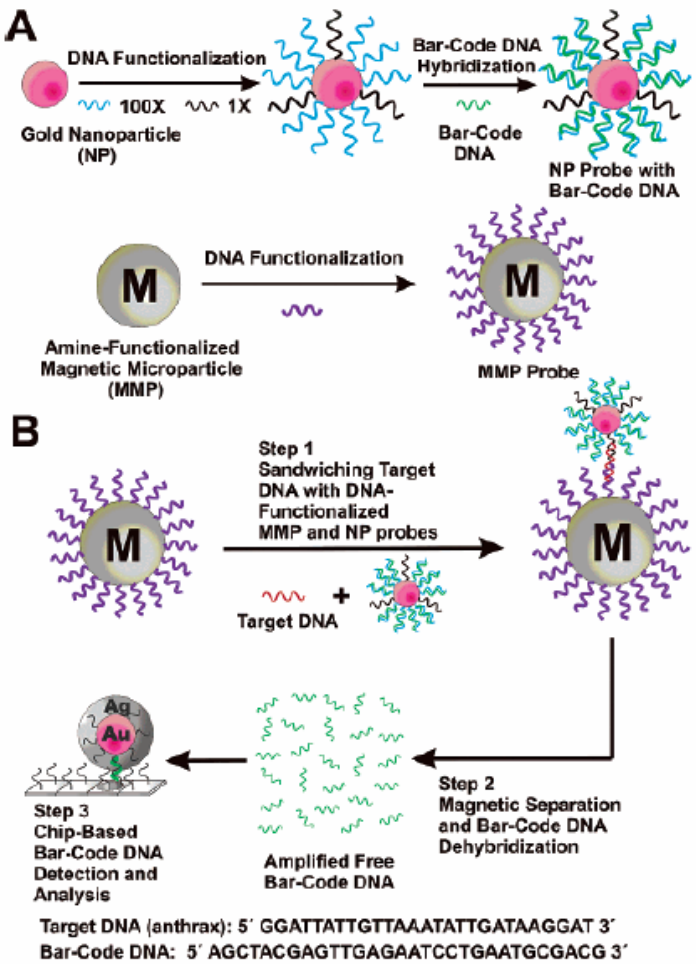

Figure 1. The DNA-BCA assay. (A) Nanoparticle and magnetic microparticle probe preparation. (B) Nanoparticle-based PCR-less DNA amplification scheme.

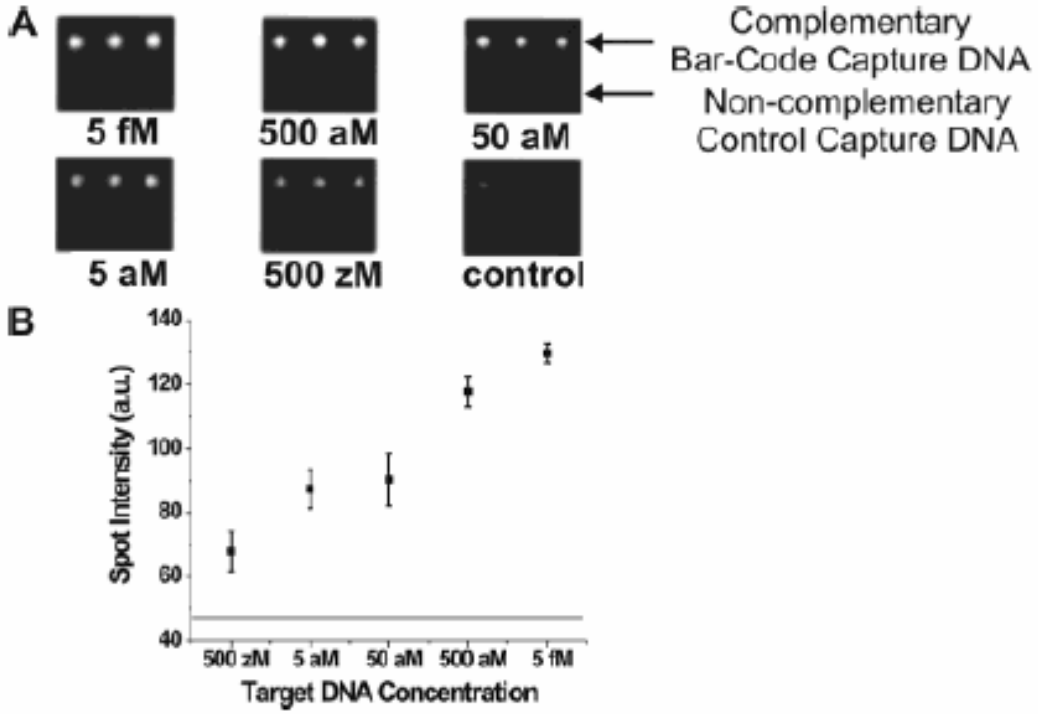

Figure 2. Amplified anthrax bar-code DNA detection with the Verigene ID system. (A) Anthrax bar-code DNA detection with 30 nm NP probes. (B) Quantitative data of spot intensities with 30 nm NP probes (Adobe Photoshop, Adobe Systems, Inc., San Jose, CA). The horizontal line represents control signal intensity (47 ± 2).

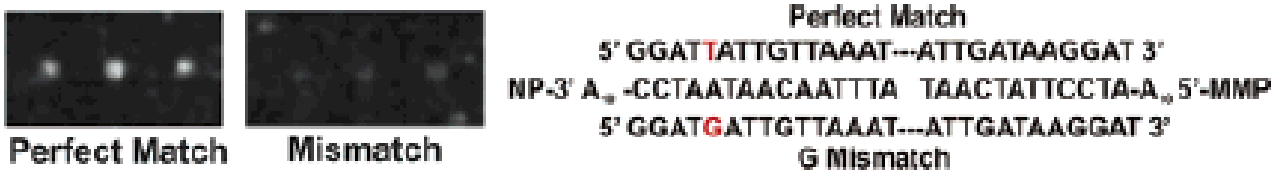

Figure 3. Single base mismatch experiment.

Nanoparticle-Based Bio–Bar Codes for the Ultrasensitive Detection of Proteins

26 SEPTEMBER 2003 VOL 301 SCIENCE

Jwa-Min Nam,* C. Shad Thaxton,* Chad A. Mirkin†

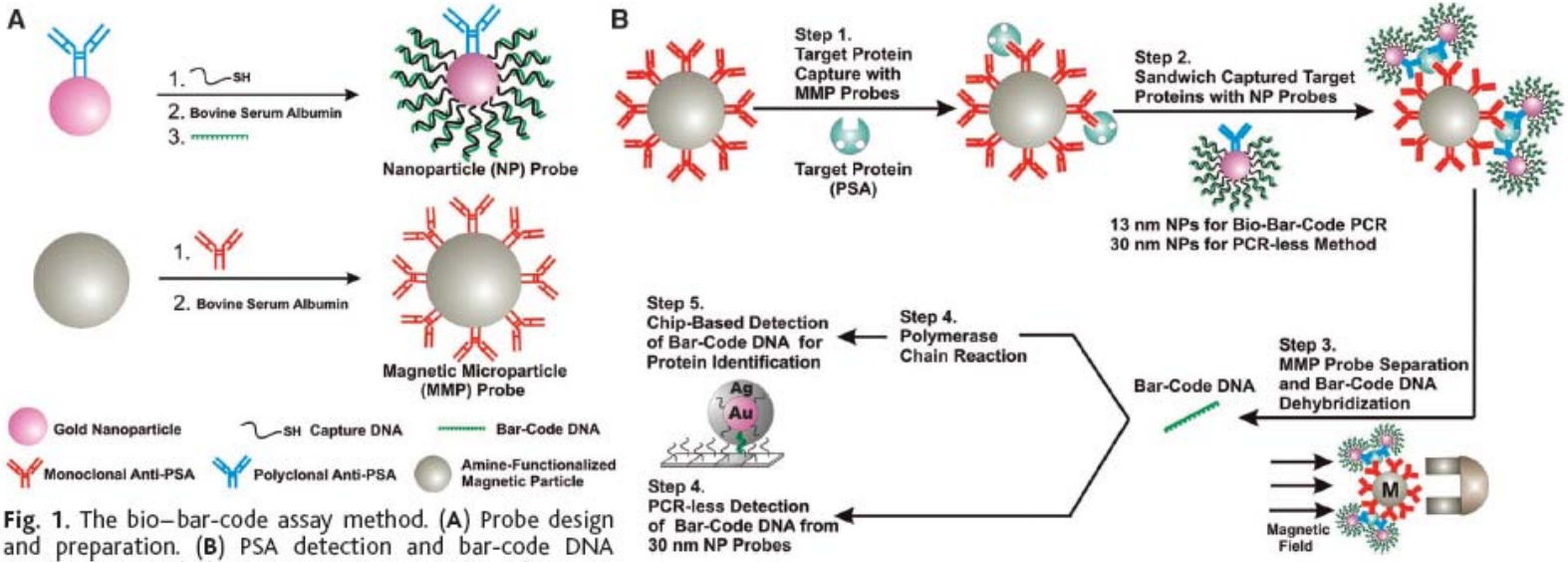

Fig. 1. The bio–bar-code assay method. (**A**) Probe design and preparation. (**B**) PSA detection and bar-code DNA amplification and identification. In a typical PSA-detection experiment, an aqueous dispersion of MMP probes functionalized with mAbs to PSA (50 μl of 3 mg/ml magnetic probe solution) was mixed with an aqueous solution of free PSA (10 μl of PSA) and stirred at 37°C for 30 min (Step 1). A 1.5-ml tube containing the assay solution was placed in a BioMag microcentrifuge tube separator (Polysciences, Incorporated, Warrington, PA) at room temperature. After 15 s, the MMP-PSA hybrids were concentrated on the wall of the tube. The supernatant (solution of unbound PSA molecules) was removed, and the MMPs were resuspended in 50 μl of 0.1 M phosphate-buffered saline (PBS) (repeated twice). The NP probes (for 13-nm NP probes, 50 μl at 1 nM; for 30-nm NP probes, 50 μl at 200 pM), functionalized with polyclonal Abs to PSA and hybridized bar-code DNA strands, were then added to the assay solution. The NPs reacted with the PSA immobilized on the MMPs and provided DNA strands for signal amplification and protein identification (Step 2). This solution was vigorously stirred at 37°C for 30 min. The MMPs were then washed with 0.1 M PBS with the magnetic separator to isolate the magnetic particles. This step was repeated four times, each time for 1 min, to remove everything but the MMPs (along with the PSA-bound NP probes). After the final wash step, the MMP probes were resuspended in NANOpure water (50 μl) for 2 min to dehybridize bar-code DNA strands from the nanoparticle probe surface. Dehybridized bar-code DNA was then easily separated and collected from the probes with the use of the magnetic separator (Step 3). For bar-code DNA amplification (Step 4), isolated bar-code DNA was added to a PCR reaction mixture (20-μl final volume) containing the appropriate primers, and the solution was then thermally cycled (*20*). The bar-code DNA amplicon was stained with ethidium bromide and mixed with gel-loading dye (*20*). Gel electrophoresis or scanometric DNA detection (*24*) was then performed to determine whether amplification had taken place. Primer amplification was ruled out with appropriate control experiments (*20*). Notice that the number of bound NP probes for each PSA is unknown and will depend upon target protein concentration.

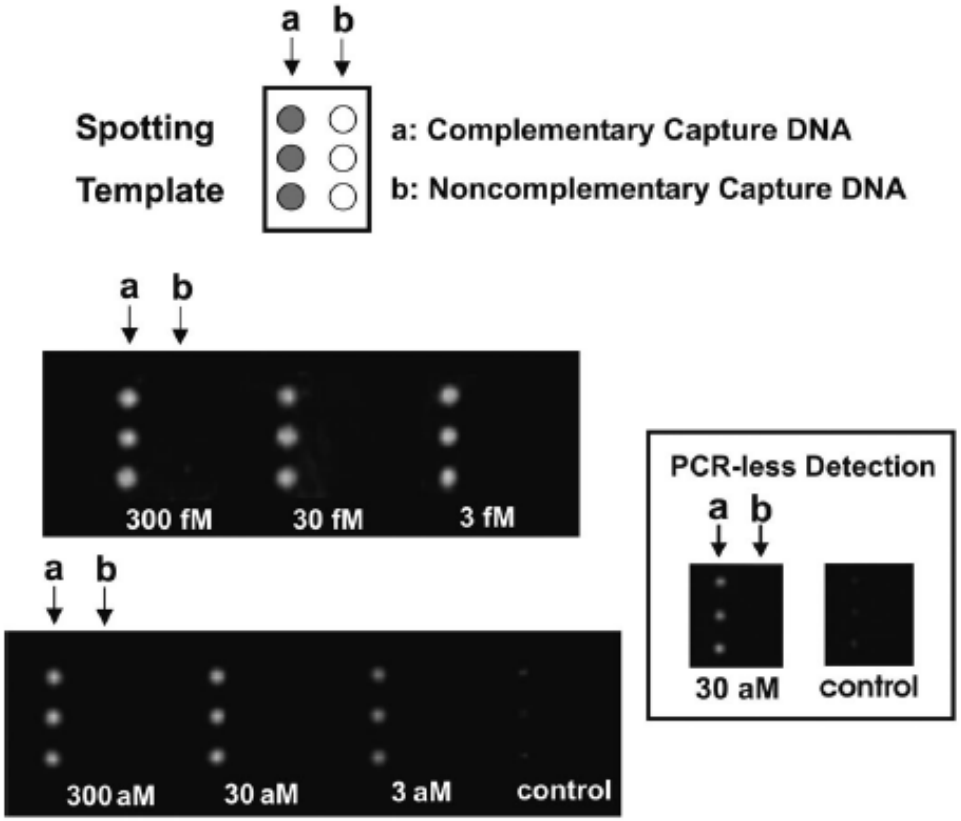

Fig. 2. Scanometric detection of PSA-specific bar-code DNA. PSA concentration (sample volume of 10 μl) was varied from 300 fM to 3 aM and a negative control sample where no PSA was added (control) is shown. For all seven samples, 2 μl of antidinitrophenyl (10 pM) and 2 μl of β-galactosidase (10 pM) were added as background proteins. Also shown is PCR-less detection of PSA (30 aM and control) with 30 nm NP probes (inset). Chips were imaged with the Verigene ID system (*20*).

Array-Based Electrical Detection of DNA with Nanoparticle Probes

So-Jung Park, T. Andrew Taton,* Chad A. Mirkin†

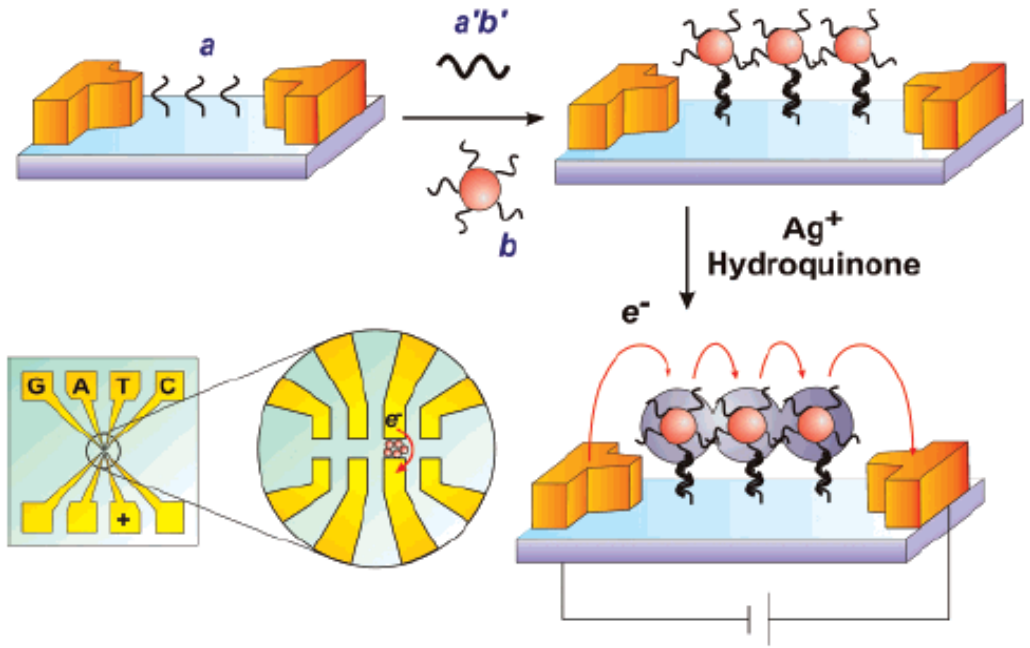

Figure 7. When the capture/target/probe sandwich is positioned in the gap between two electrodes, catalytic reduction of silver onto the sandwich system results in a signal that can be detected electrically. (Reprinted with permission from *Science* (http://www.aaas.org), ref 93. Copyright 2002 American Association for the Advancement of Science.)

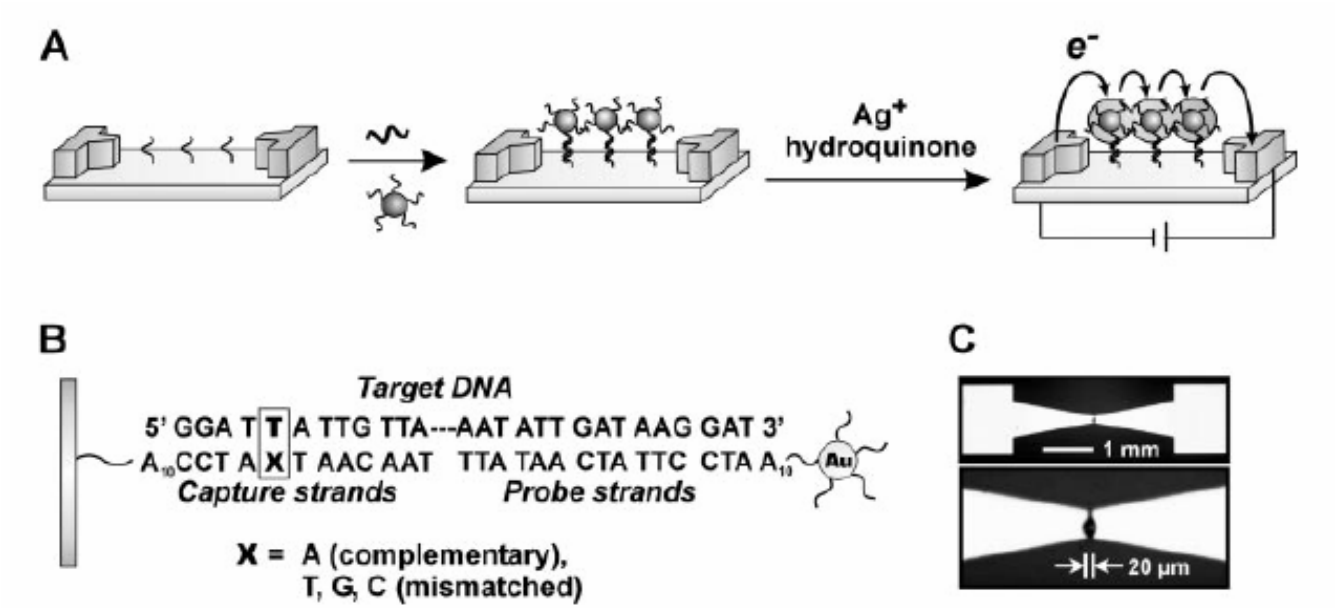

Fig. 1. (**A**) Scheme showing concept behind electrical detection of DNA. (**B**) Sequences of capture, target, and probe DNA strands. (**C**) Optical microscope images of the electrodes used in a typical detection experiment. The spot in the electrode gap in the high-magnification image is food dye spotted by a robotic arrayer (GMS 417 Microarrayer, Genetic Microsystems, Woburn, MA).

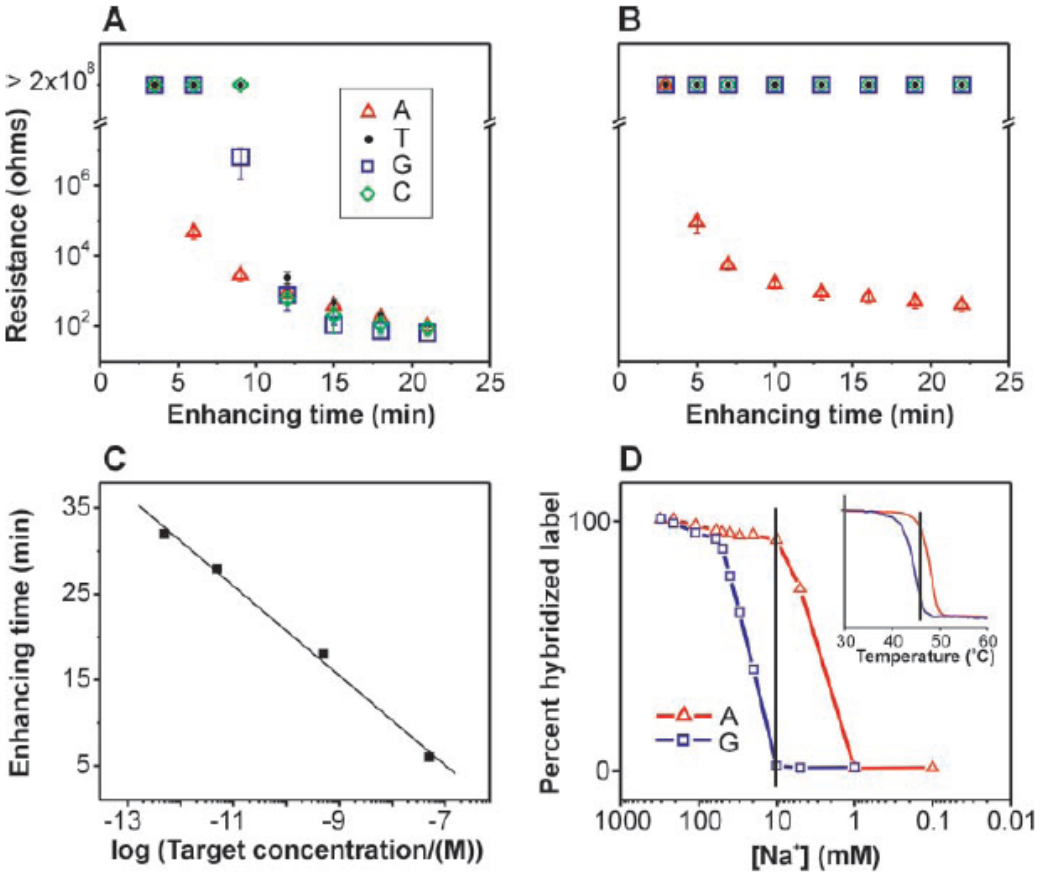

Fig. 2. Resistance of the electrode arrays measured as a function of increasing silver enhancing time (**A**) without and (**B**) with washing with 0.01 M PBS at room temperature before silver enhancing. (**C**) A graph of the silver enhancing time required to reach a resistance value of 100 kilohm as a function of target concentration showing that target can be detected in the 50 nM to 500 fM concentration range by adjusting silver enhancing time. Target DNA and nanoparticle probes were cohybridized to capture strand DNA in 0.6 M PBS for 6 hours in all quantification experiments; this procedure leads to slightly greater sensitivity than the aforementioned protocol. (**D**) DNA duplex denaturation curve as a function of $[Na^+]$ for the perfectly complementary oligonucleotide (X = A) and the strand with a wobble mismatch (X = G). For these experiments, the inside walls of glass cuvettes (Fisher Scientific, Pittsburgh, PA) were functionalized with the appropriate capture-strand oligonucleotide and then treated with 0.3 M PBS solution of target DNA (10 nM) for 10 hours followed by nanoparticle probes (2 nM) for 5 hours. The extinction at 520 nm (1:1 correlation with "% hybridized label") was monitored after washing the cuvettes with a series of buffer solutions containing different NaCl concentrations (*20*). (**Inset**) Thermal-denaturation curves for the perfectly matched DNA (X = A) and the one with a wobble mismatch (X = G).

Magnetic Separation

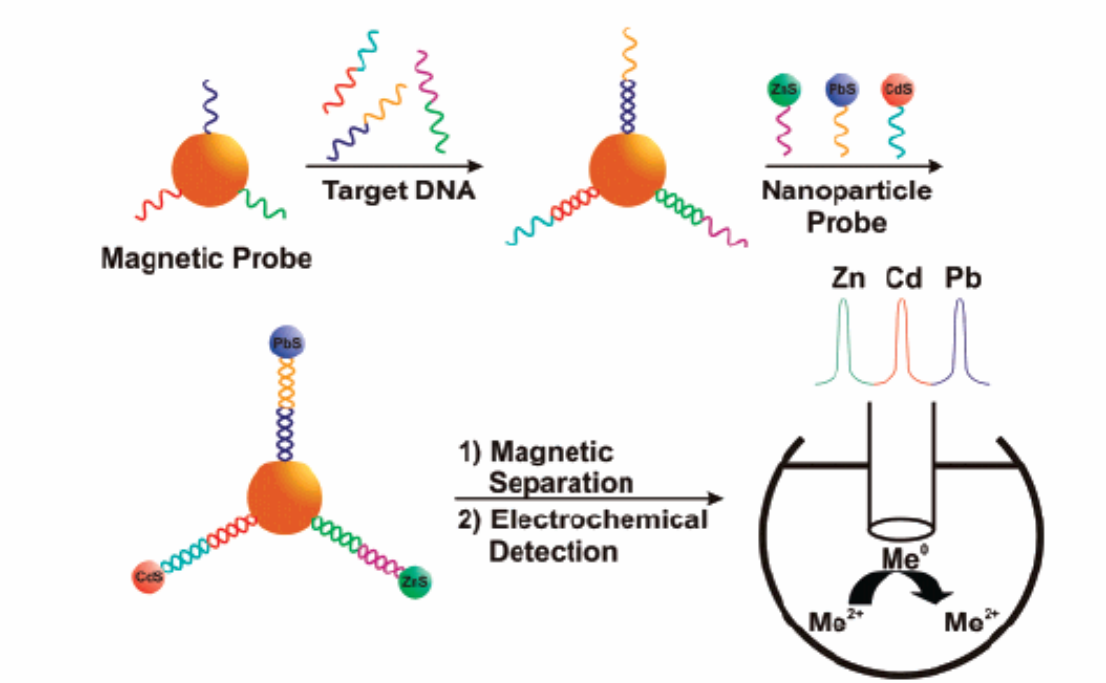

Figure 8. Magnetic microparticles (large brown spheres) labeled with DNA capture strands can bind target DNA, and then oligonucleotide-functionalized nanoparticle labels (small spheres) with different electrochemical signatures can be used to code for the specific target DNA of interest.

Magnetic Relaxation

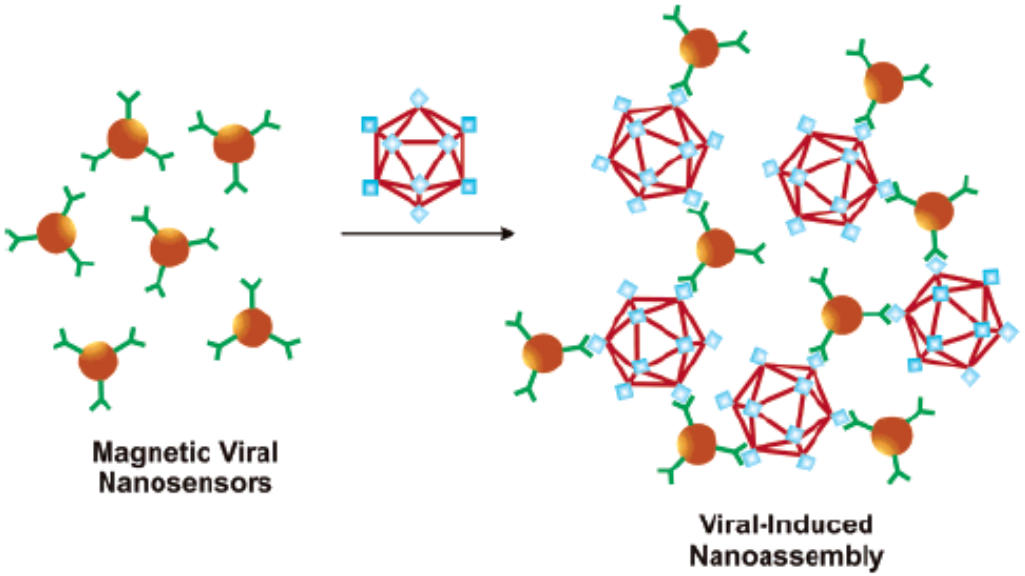

Figure 9. Superparamagnetic iron oxide nanoparticles (brown spheres) labeled with antibodies (green) specific to antigens (blue) presented on viral capsids (red) will form aggregates in the presence of target viruses, which result in detectable perturbations of the T_2 magnetic relaxation times of protons in the surrounding media.

"Dip-Pen" Nanolithography

Richard D. Piner, Jin Zhu, Feng Xu, Seunghun Hong, Chad A. Mirkin*

SCIENCE VOL 283 29 JANUARY 1999

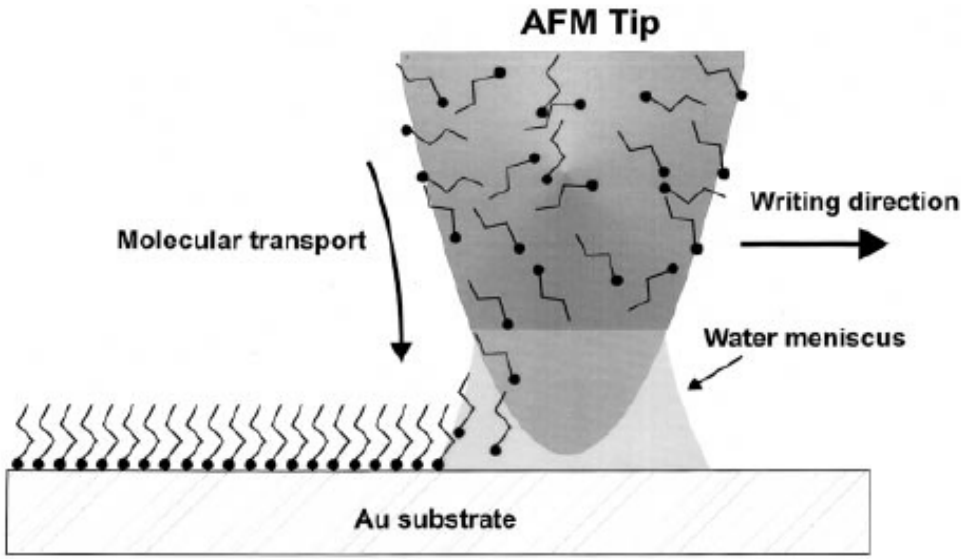

Fig. 1. Schematic representation of DPN. A water meniscus forms between the AFM tip coated with ODT and the Au substrate. The size of the meniscus, which is controlled by relative humidity, affects the ODT transport rate, the effective tip-substrate contact area, and DPN resolution.

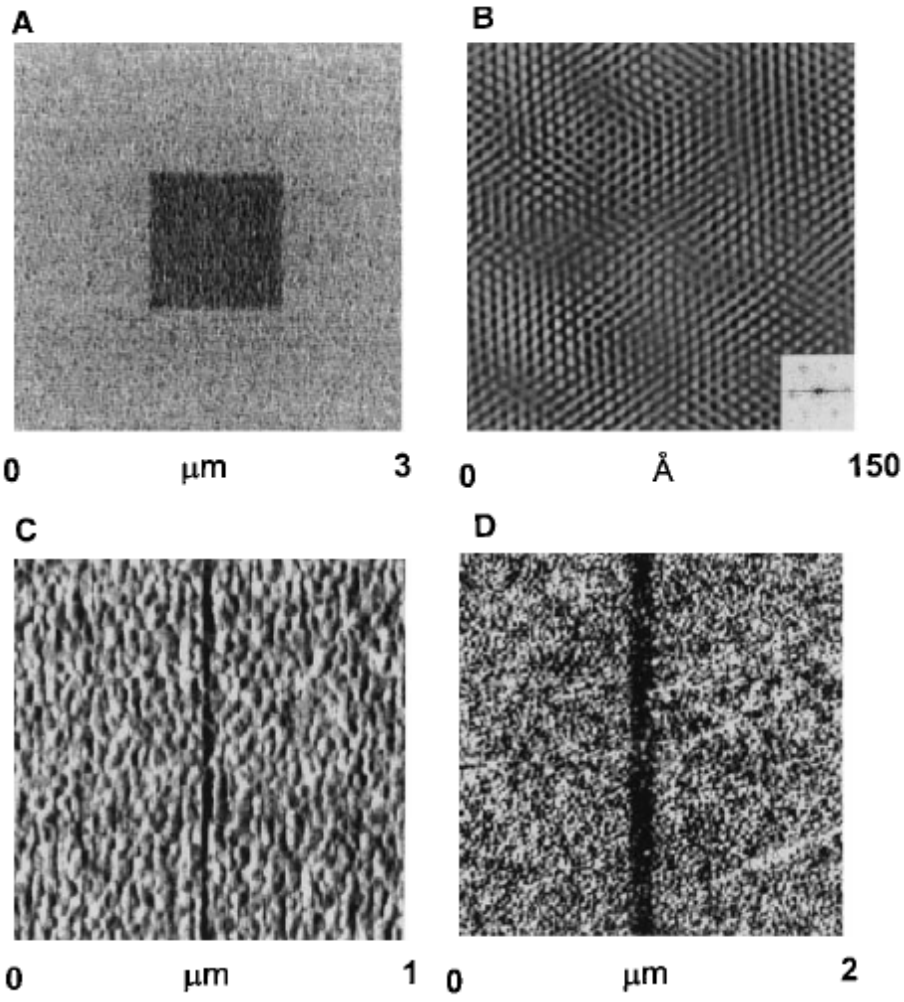

Fig. 2. (**A**) Lateral force image of a square of ODT measuring 1 μm by 1 μm, deposited onto a Au substrate by DPN. This pattern was generated by scanning the 1-μm^2 area at a scan rate of 1 Hz for a period of 10 min at a relative humidity of 39%. Then the scan size was increased to 3 μm, and the scan rate was increased to 4 Hz while the image was recorded. The faster scan rate prevents ODT transport. (**B**) Lattice-resolved, lateral force image of an ODT SAM deposited onto Au(111)/mica by DPN. The image has been filtered with a fast Fourier transform (FFT), and the FFT of the raw data is shown in the lower right insert. The monolayer was generated by scanning a 1000 Å square area of the Au(111)/mica five times at a rate of 9 Hz at 39% relative humidity. (**C**) Lateral force image of a 30-nm-wide line (3 μm long) deposited onto Au/mica by DPN. The line was generated by scanning the tip in a vertical line repeatedly for 5 min at a scan rate of 1 Hz. (**D**) Lateral force image of a 100-nm line deposited on Au by DPN. The method of depositing this line is analogous to that used to generate the image in (*C*), but the writing time was 1.5 min. In all images, darker regions correspond to areas of relatively lower friction.

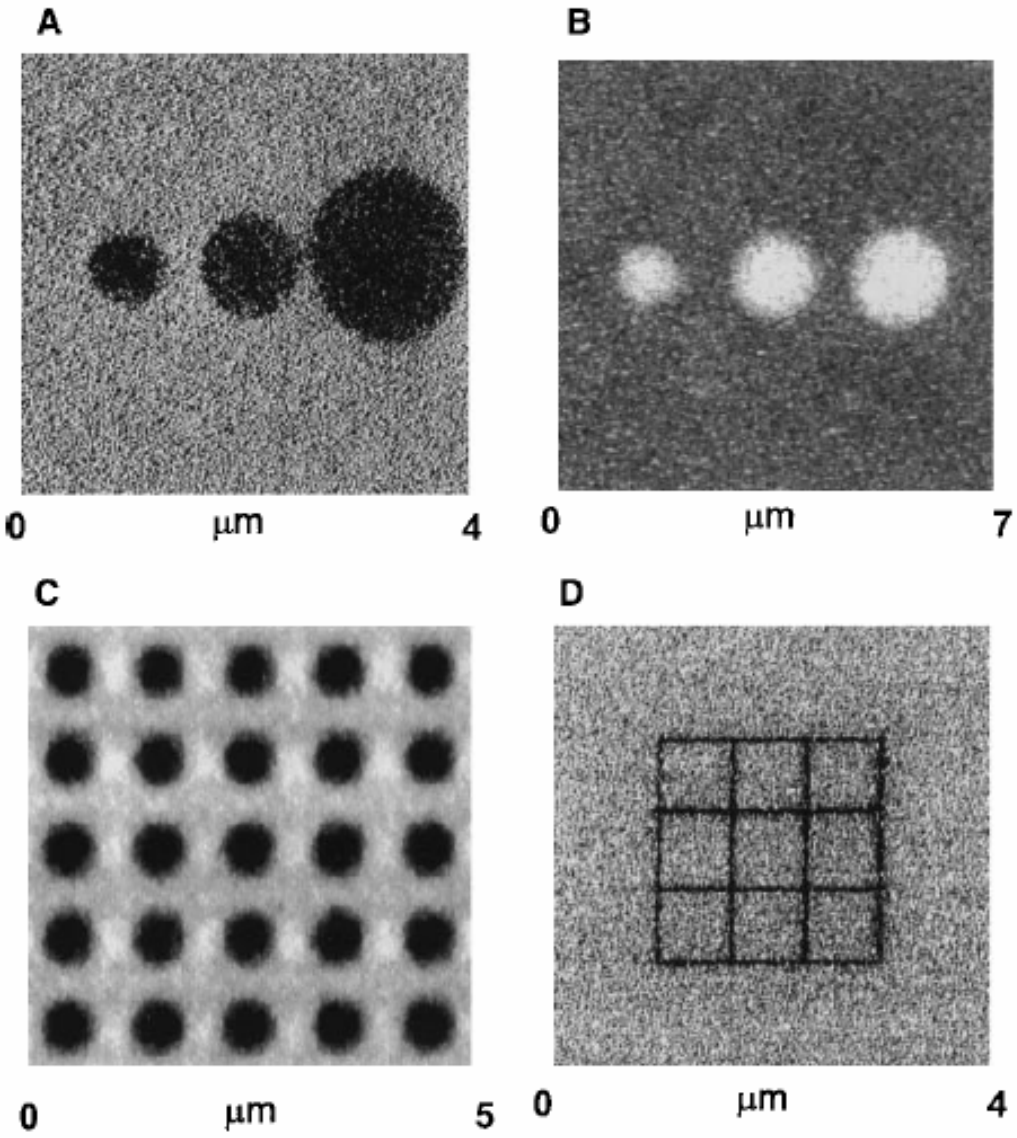

Fig. 3. (**A**) Lateral force image of an Au substrate after an AFM tip, which was coated with ODT, had been in contact with the substrate for 2, 4, and 16 min (left to right); the relative humidity was held constant at 45%, and the image was recorded at a scan rate of 4 Hz. (**B**) Lateral force image of dots of 16-mercaptohexadecanoic acid on a Au substrate. To generate the dots, an AFM tip coated with 16-mercaptohexadecanoic acid was held on the Au substrate for 10, 20, and 40 s (left to right). The relative humidity was 35%. The images show that the transport properties of 16-mercaptohexadecanoic acid and of ODT differ substantially. (**C**) Lateral force image of an array of dots generated by DPN. Each dot was generated by holding an ODT-coated tip in contact with the surface for ~20 s. Writing and recording conditions were the same as in (A). (**D**) Lateral force image of a molecule-based grid. Each line is 100 nm in width and 2 μm in length and required 1.5 min to write.

A Nanoplotter with Both Parallel and Serial Writing Capabilities

Seunghun Hong and Chad A. Mirkin*

9 JUNE 2000 VOL 288 SCIENCE

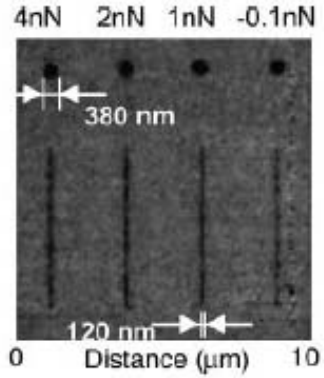

Fig. 1. Lateral force microscopy (LFM) images of ODT monolayer nanodot and line features on gold generated by the same tip but under different tip-substrate contact forces. Feature sizes vary less than 10%.

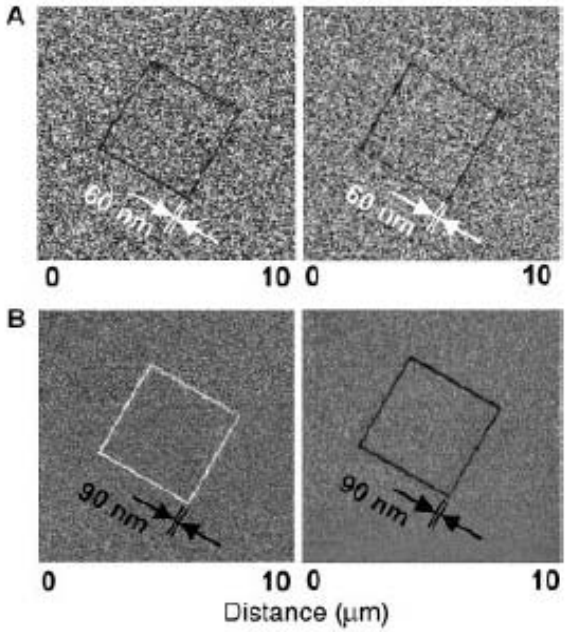

Fig. 2. Parallel DPN writing using two tips and a single feedback system. (**A**) Two nearly identical ODT patterns generated on gold in parallel fashion with a two-pen cantilever. (**B**) Two nearly identical patterns generated on gold in parallel fashion with a two-pen cantilever with each pen coated with a different ink. The pattern on the left was generated from an MHA-coated tip and exhibits a higher lateral force than the gold substrate. The pattern on the right was generated with an ODT-coated tip and exhibits a lower lateral force than the gold substrate.

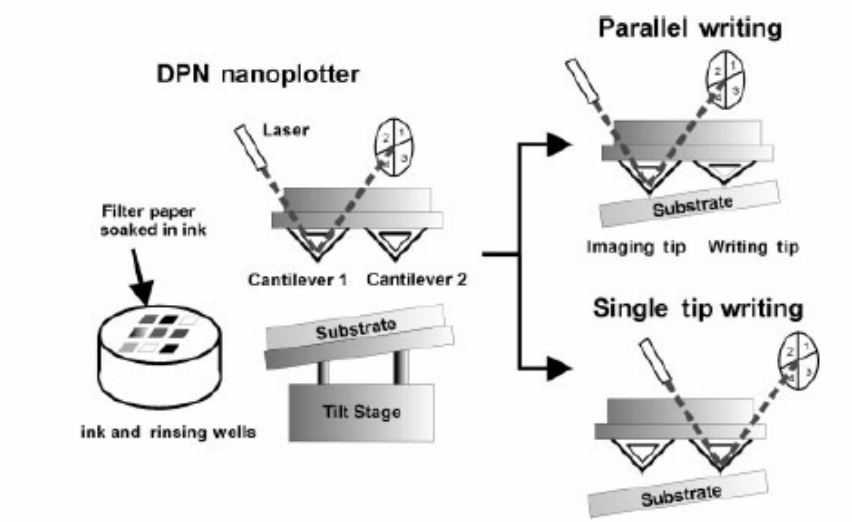

Fig. 4. LFM images of eight identical patterns generated with one imaging tip and eight writing tips coated with ODT molecules.

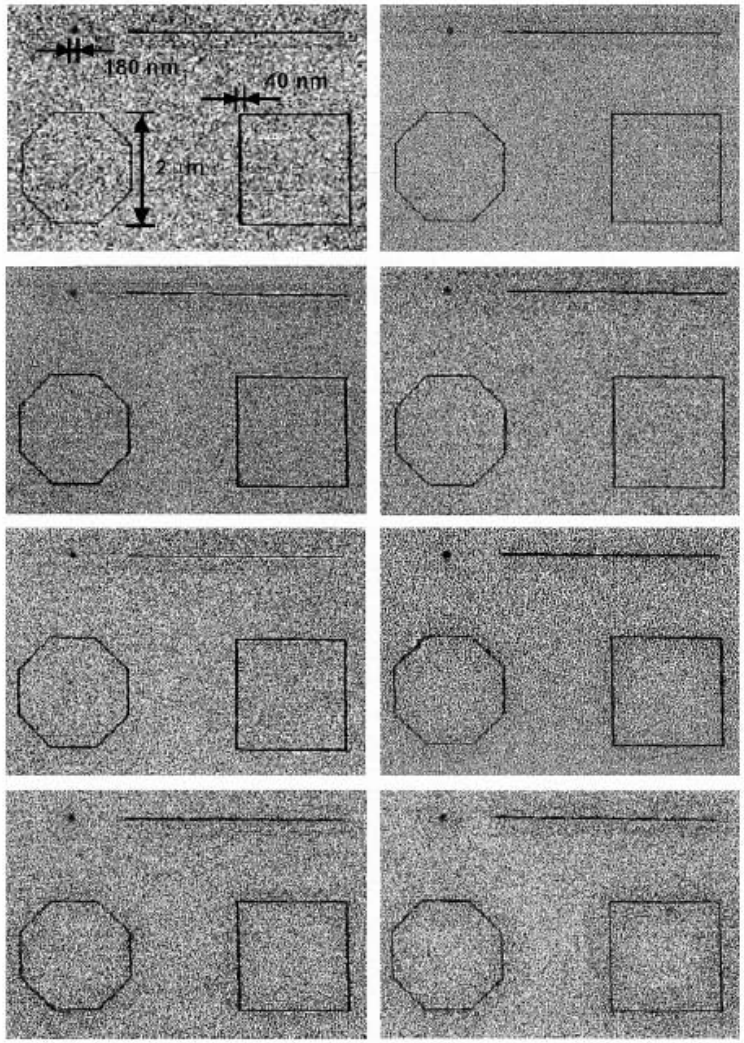

Protein Nanoarrays Generated By Dip-Pen Nanolithography

Ki-Bum Lee,[1] So-Jung Park,[1] Chad A. Mirkin,[1]* Jennifer C. Smith,[2] Milan Mrksich[2]*

1 MARCH 2002 VOL 295 SCIENCE

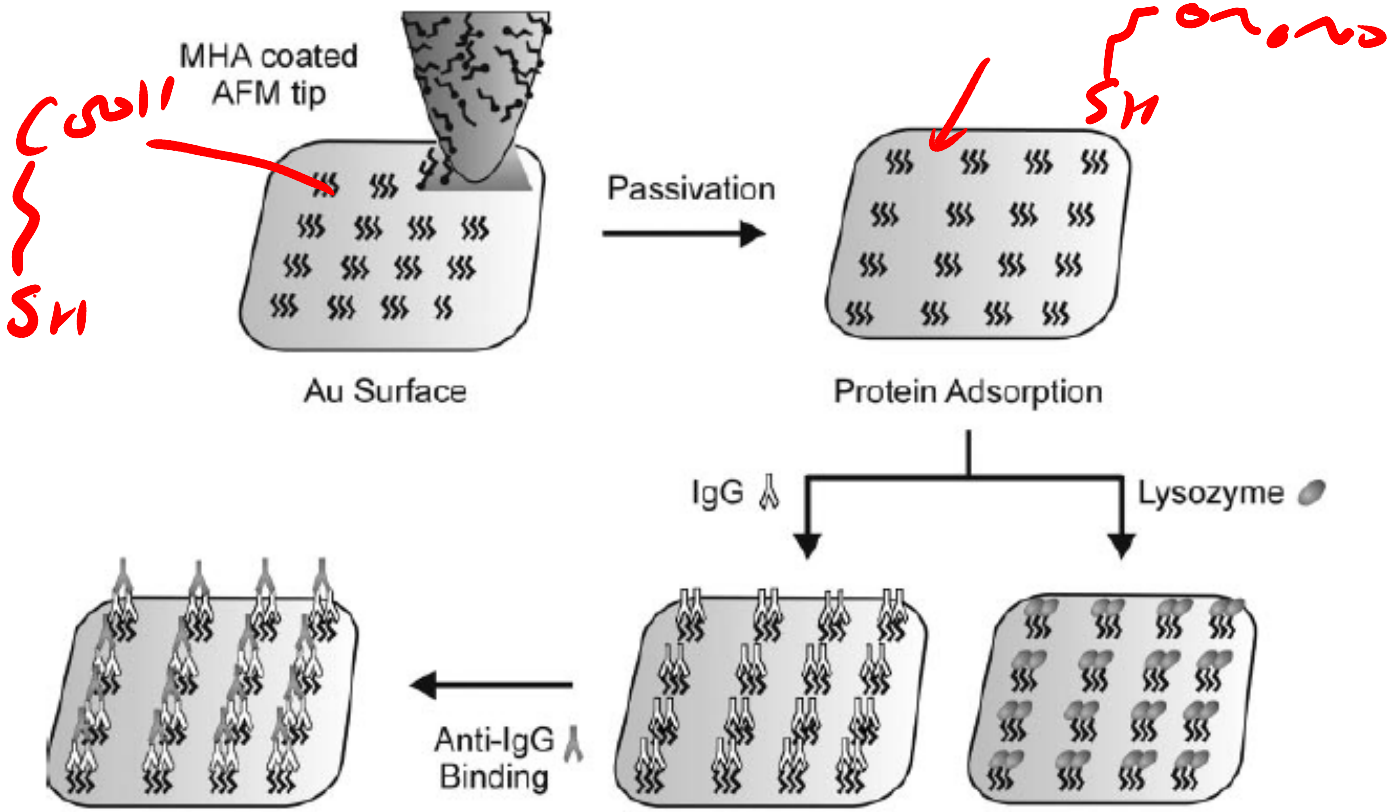

Fig. 2. Diagram of proof-of-concept experiments, in which proteins were absorbed on preformed MHA patterns. The resulting protein arrays were then characterized by AFM.

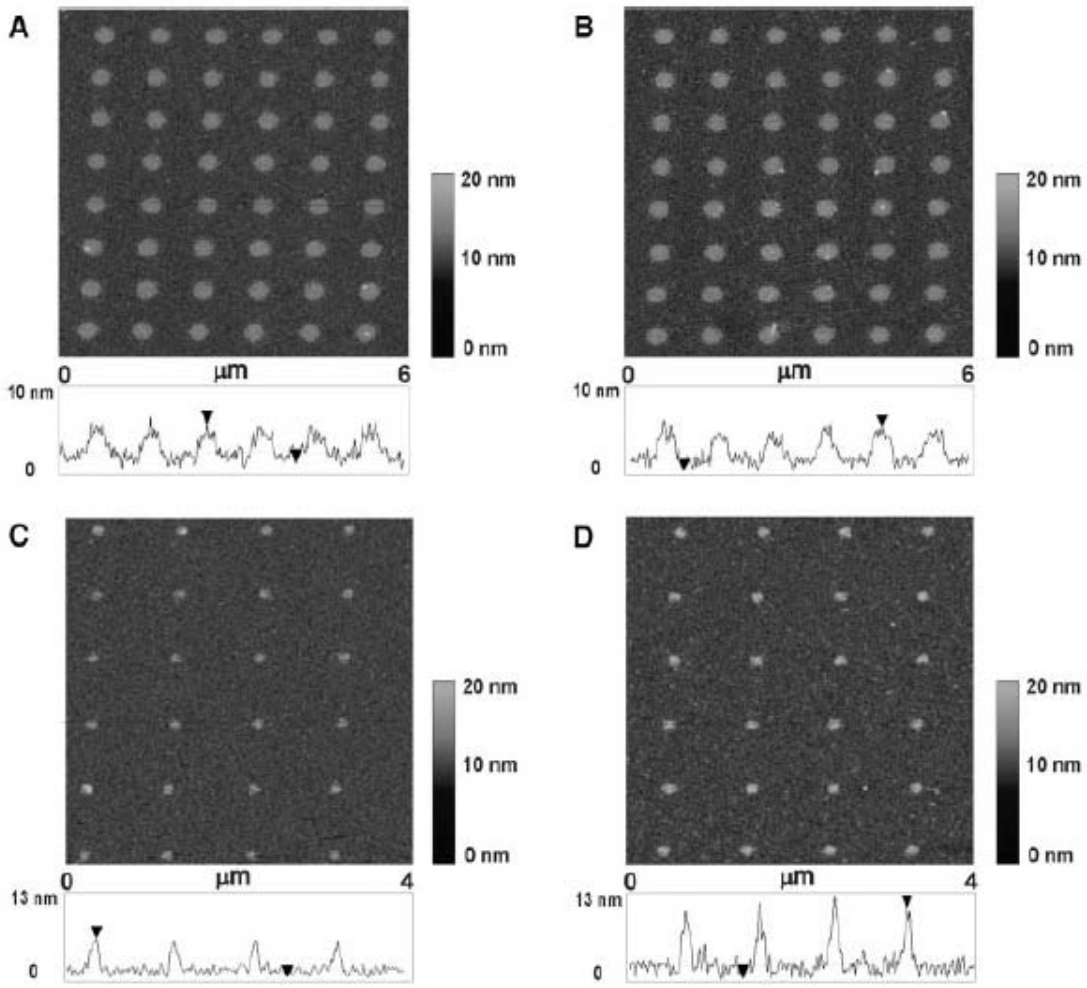

Fig. 3. AFM tapping mode image and height profile of rabbit IgG assembled onto an MHA dot array generated by DPN before (**A**) and after (**B**) exposure to a solution containing lysozyme, Retronectin, goat/sheep anti-IgG, and human anti-IgG. An IgG nanoarray before (**C**) and after (**D**) treatment with a solution containing lysozyme, goat/sheep anti-IgG, human anti-IgG, and rabbit anti-IgG. All images were taken at a 0.5-Hz scan rate in tapping mode.

Direct Patterning of Modified Oligonucleotides on Metals and Insulators by Dip-Pen Nanolithography

L. M. Demers,* D. S. Ginger,* S.-J. Park, Z. Li, S.-W. Chung, C. A. Mirkin†

7 JUNE 2002 VOL 296 SCIENCE

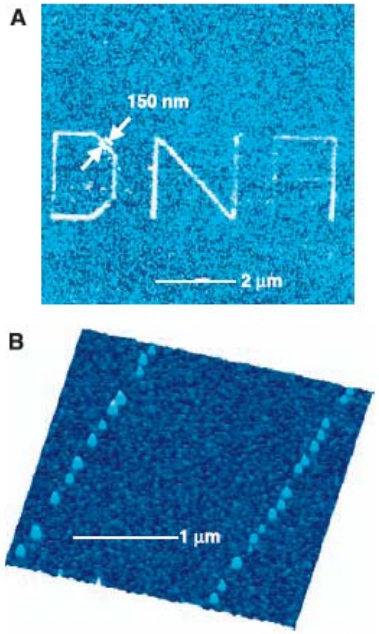

Fig. 1. Direct transfer of DNA onto gold substrates by DPN. (**A**) Tapping-mode AFM image of hexanethiol-modified oligonucleotides patterned on polycrystalline gold. The scale bar represents 2 μm, and the space between the arrows is 150 nm. (**B**) Tapping-mode AFM image of single oligonucleotide-modified gold nanoparticles (13-nm diameter) bound to a high-resolution DNA line on gold by Watson-Crick base pairing in the presence of complementary linking DNA. The scale bar represents 1 μm.

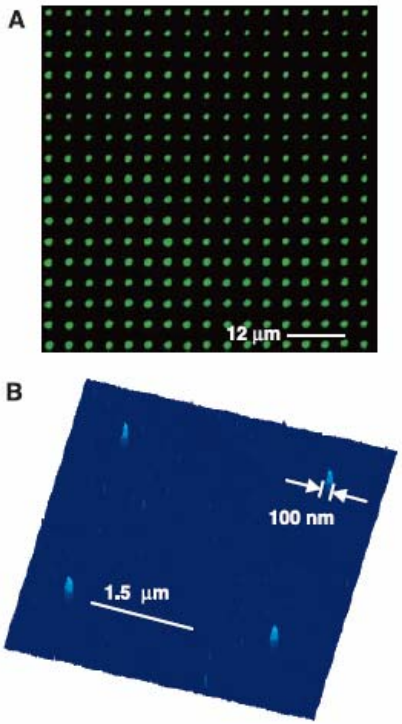

Fig. 2. Direct DPN transfer of DNA onto insulating substrates. (**A**) Epifluorescence micrograph of fluorophore-labeled DNA (Oregon Green 488-X) hybridized to a DPN-generated pattern of complementary oligonucleotides on an SiO_x surface. The scale bar represents 12 μm. (**B**) Tapping-mode AFM image of oligonucleotide-modified gold nanoparticles (13-nm diameter) hybridized to a second, high-resolution pattern after removal (using DI water) of the fluorophore-labeled DNA. The scale bar represents 1.5 μm, and the space between the arrows is 100 nm.

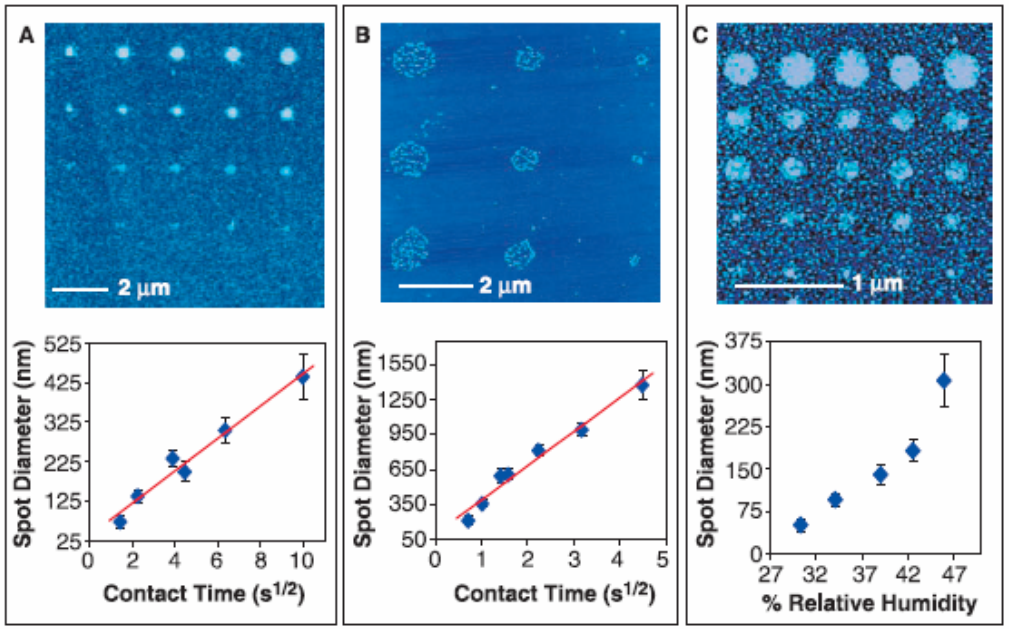

Fig. 3. DPN control over deposited feature size. (**A**) Tapping-mode AFM image of thiol-modified DNA spotted on a gold substrate for different contact times at 45% relative humidity (top) and plot of dot diameter versus square root of contact time (bottom). (**B**) Tapping-mode AFM image of nanoparticles hybridized to DNA spots formed on SiO_x for different contact times at 45% relative humidity (top) and plot of dot diameter versus square root of contact time (bottom). The scale bars for (A) and (B) represent 2 μm. (**C**) Tapping-mode AFM image of DNA spots generated on polycrystalline Au with a contact time of 10 s per spot, at varying relative humidity (top), and a plot of spot diameter versus relative humidity (bottom). The scale bar represents 1 μm. Error bars for all plots were calculated from the standard deviation of at least five points.

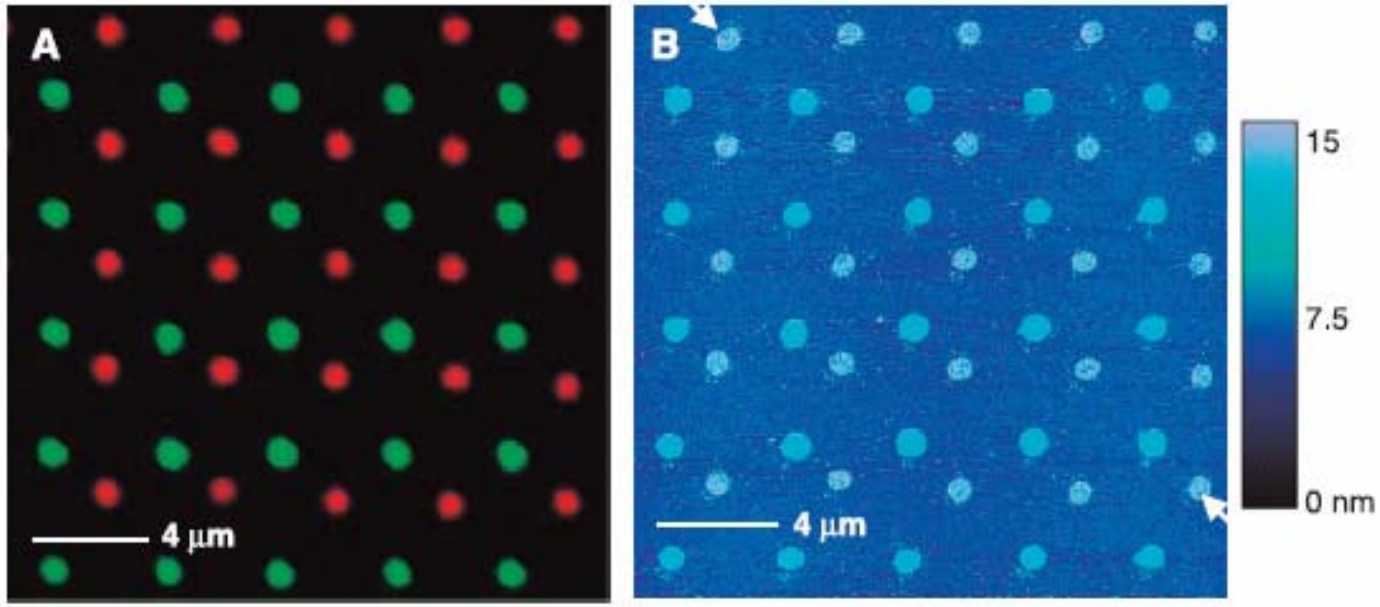

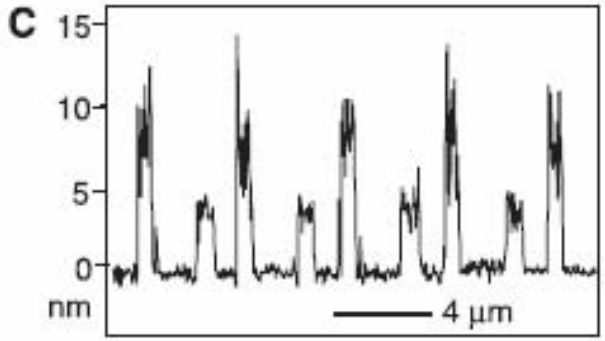

Fig. 4. Direct patterning of multiple-DNA inks by DPN. (**A**) Combined red-green epifluorescence image of two different fluorophore-labeled sequences (Oregon Green 488-X and Texas Red-X) simultaneously hybridized to a two-sequence array deposited on an SiO_x substrate by DPN. (**B**) Tapping-mode AFM image of 5 (dark)- and 13 (light)-nm–diameter gold nanoparticles assembled on the same pattern after dehybridization of the fluorophore-labeled DNA. The scale bars represent 4 μm. (**C**) The line plot was taken diagonally through both nanoparticle patterns, and the start and finish are indicated by the arrows in (B). The scale bar represents 4 μm.

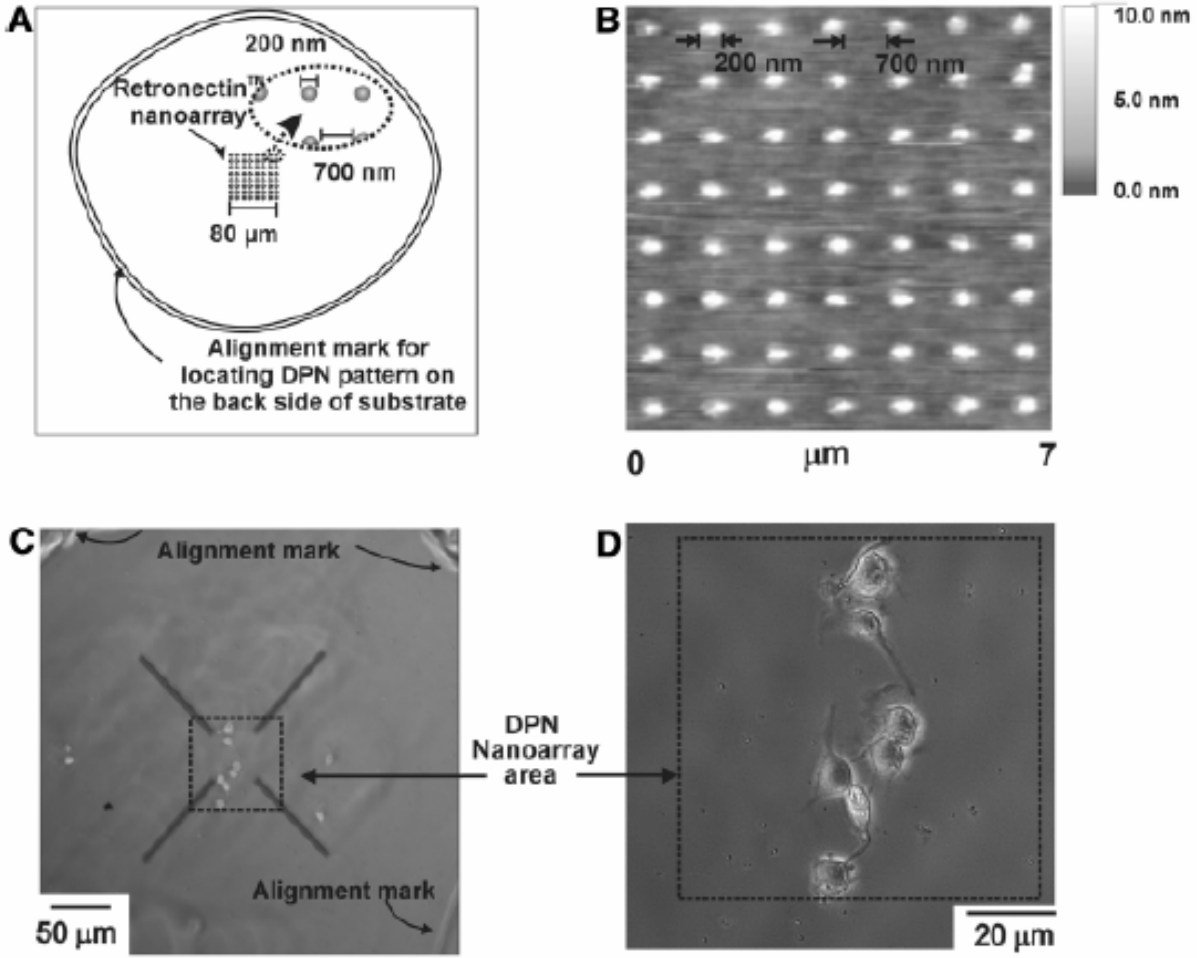

Fig. 4. (**A**) Diagram describing the cell adhesion experiment on the DPN-generated pattern. The total patterned area is 6400 μm^2. The alignment marks were generated by scratching a circle into the backside of the Au-coated glass substrate. (**B**) Topography image (contact mode) of the Retronectin protein array. Imaging conditions were the same as in Fig. 1B. (**C**) Large-scale optical microscope image showing the localization of cells in the nanopatterned area. (**D**) Higher resolution optical image of the nanopatterned area, showing intact cells.

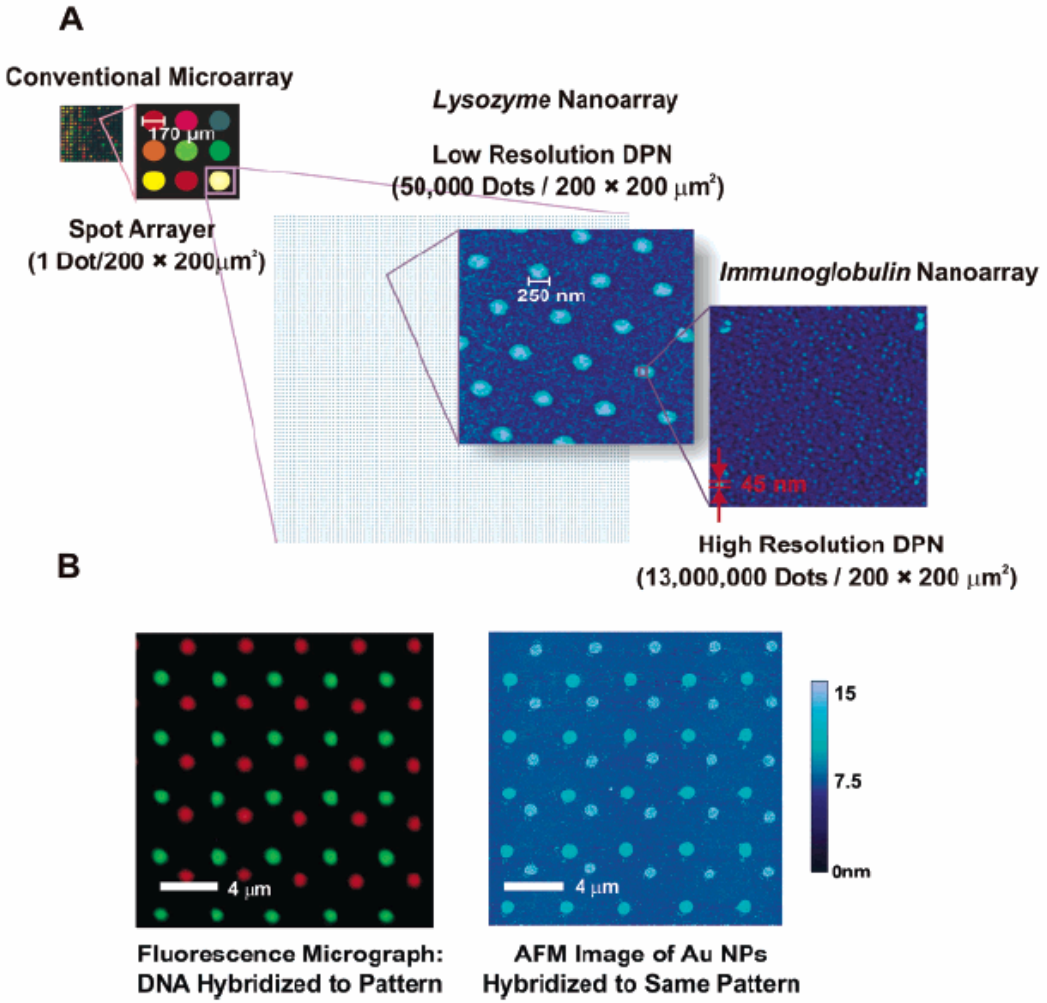

Figure 10. In a conventional microarray spot sizes are typically 200 × 200 μm^2. Using low-resolution dip-pen nanolithography (DPN), 50 000 250-nm protein spots can be spotted in an equivalent area. Patterns can be further miniaturized using high-resolution DPN to generate a total of 13 000 000 spots in a 200 × 200 μm^2 area (A). Similarly, DPN can be used to construct nanopatterns of oligonucleotides on SiO_x surfaces. The reactivity of the patterns can be interrogated using either fluorescence microscopy or atomic force microscopy (AFM) (B). (Reprinted with permission from *Science* (http://www.aaas.org), ref 114. Copyright 2002 American Association for the Advancement of Science.)

Table 1. Detection Limits of Nucleic Acid Assays[a]

	assay	ss DNA	PCR products	genomic DNA
nanostructure-based methods	colorimetric[29] (cross-linked Au nanoparticles)	~10 nM		
	colorimetric[36] (non-cross-linked Au nanoparticles)	60 nM		
	magnetic relaxation[97] (iron oxide nanoparticles)	20 pM		
	electrochemical[96] (nanoparticles)	270 pM		
	scanometric[35,66,67] (Au nanoparticles with Ag amplification)	50 fM	100 aM[b]	200 fM
	Raman spectroscopy[68] (Au nanoparticles with Ag amplification)	~1 fM		
	electrical[93] (Au nanoparticles with Ag amplification)	500 fM		
	electrical[99] (Si nanowire)	10 fM		
	electrical[103] (carbon nanotube)	54 aM		
	resonant light-scattering[61−66] (metal nanoparticles)	170 fM[b]		33 fM
	fluorescence[56] (ZnS and CdSe quantum dots)	2 nM		
	surface plasmon resonance[41] (Au nanoparticles)	10 pM		
	quartz crystal microbalance[94] (Au nanoparticles)	~1 fM		
	laser diffraction[42] (Au nanoparticles)	~50 fM		
	fluorescence[45] (fluorescent nanoparticles)	~1 fM		
	bio-bar-code amplification[71] (Au nanoparticles with Ag amplification)	500 zM		
other non-enzymatic based methods	fluorescence[35] (molecular fluorophores)		~600 fM[b]	
	fluorescence (dendrimer amplification)[134]		2.5 μg	
	electrochemical amplification[136] (electroactive reporter molecules)	100 aM		

[a] Detection limits can vary based on target length and sequence; therefore, it is difficult to compare assays without testing them using identical targets and conditions. [b] Values taken from ref 34.

Table 2. Detection Limits of Protein Assays

	assay	target	protein in saline	protein in serum
nanostructure-based methods	optical[72] (Au nanoshells)	rabbit IgG	0.88 ng/mL (~4.4 pM)[a]	0.88 ng/mL (~4.4 pM)[a]
	optical[74] (Au nanoparticles)	IgE and IgG1	~20 nM	
	magnetic relaxation[98] (iron oxide nanoparticles)	adenovirus (ADV) and herpes simplex virus (HSV)	100 ADV/ 100μL	50 HSV/ 100 μL
	scanometric[79] (Au nanoparticles with Ag amplification)	mouse IgG	200 pM	
	Raman[82] (Au nanoparticles with Raman labels)	prostate-specific antigen		30 fM
	surface plasmon resonance[83,84] (triangular Ag particles on surfaces)	streptavidin(S A) and anti-biotin (AB)	~1 pM SA and ~700 pM AB	
	electrical[110] (single-walled carbon nanotubes)	10E3 antibody to U1A RNA splicing factor	~1 nM	
	electrical[20] (Si nanowires)	streptavidin	10 pM	
	bio-bar-code amplification[75] (Au nanoparticles with Ag amplification)	prostate-specific antigen	30 aM (3 aM)[b]	(30 aM)[b]
molecular fluorophore methods	enzyme-linked immunosorbent assay	various	pM range	pM range
electrochemical methods	electrochemical amplification[137] (oligonucleotide reporter molecules)	IgG	13 fM	
enzyme-based amplification methods	immuno-PCR[76]	bovine serum albumin	2 fM	
	rolling circle amplification[77]	prostate-specific antigen	3 fM	

[a] Reported in ng/mL; authors converted to molar concentration for ease of comparison. [b] These values are the lower limits when PCR is used to amplify the bar-code DNA prior to scanometric detection of bar codes.